

## Flux-tube model for hadrons in QCD

Nathan Isgur

*Department of Physics, University of Toronto, Toronto, Canada M5S 1A7*

Jack Paton

*Department of Theoretical Physics, University of Oxford, 1 Keble Road, Oxford, England OX1 3NP*

(Received 30 August 1984)

We extract from the strong-coupling Hamiltonian lattice formulation of QCD a model for hadrons based on the use of quark and flux-tube degrees of freedom. The ordinary quark model of mesons and baryons is recovered as an appropriate limit, but the properties of hybrids, pure glue, and multi-quark hadrons are also predicted by the model. The basic tenets of the model can be tested by lattice Monte Carlo simulations.

### I. INTRODUCTION

Although QCD seems to be the correct theory of the strong interactions,<sup>1</sup> its application to the main phenomena of strong-interaction physics, such as hadron masses and hadron decay and production characteristics, is still in a rudimentary state. Lattice simulations have now given a convincing demonstration that QCD confines, but attempts to calculate the masses of the low-lying mesons and baryons on the lattice, while qualitatively encouraging, have not yet reached a satisfactory conclusion.<sup>2</sup> It is unclear, moreover, how much further these *ab initio* calculations can be taken with foreseeable computer capacity.

By contrast, the quark model has had considerable success in systematizing many of the details of meson and baryon spectra, intrinsic moments, and couplings, especially after the naive quark model was supplemented<sup>3</sup> with certain simple dynamical features characteristic of QCD. In this form the quark model has even been applied with some success to such complicated problems as deriving the nucleon-nucleon potential which underlies nuclear physics.

We present here a model for hadrons extracted from the strong-coupling Hamiltonian lattice formulation<sup>4</sup> of QCD. The model contains the ordinary quark model in an appropriate limit, but it includes as well pure glue states, hybrids (which have both quark and gluonic degrees of freedom in evidence), and other exotics. The model is not QCD, but it may be useful as a guide in the present period where rigorous solutions of QCD are unavailable. Indeed, given its complexity, we will probably always want to have models which can provide simple pictures of the dynamics of QCD, so we do not view such model building as having only temporary value.

We should stress that the spectrum of QCD will inevitably be richer than that of the naive quark model. For example, even if we remove the quarks from QCD, there would remain a nontrivial SU(3) Yang-Mills theory which must have its own spectrum of states. These states, possibly transformed in various ways by the presence of quarks, will become the "glueball" states of QCD. It is, however, unclear how the quark model should be extended

to incorporate such gluonic degrees of freedom. One widely adopted approach is to proceed by analogy with the "constituent quark" to posit the existence of a "constituent gluon" with the quantum numbers ( $J^{PC}=1^{--}$ , color octet) of a gluon of weak-coupling perturbation theory.<sup>5</sup> We pursue the opposite point of view in this paper, basing our picture on QCD in the strong-coupling regime in which the gluonic degrees of freedom have condensed into collective stringlike flux tubes. It seems to us plausible that the strong-coupling limit in which quarks are confined may be more relevant to an understanding of hadrons than the weak-coupling limit in which they are free. At any rate, it certainly seems to us worth pursuing the implications of the fact that in strong coupling there is no direct analog of the gluon, though there is of the quark.

This observation, that in strong coupling quarks and flux tubes are the natural degrees of freedom, is basic to our model. A flux tube (or "flux link" on the lattice) is a directed element (or "string") in which the scalar quantity  $\sum_{a=1}^8 \mathbf{E}_a$ <sup>2</sup> (where  $\mathbf{E}_a$  is the color-electric field) has a definite nonzero eigenvalue. As we shall see below, a quark (antiquark) acts as a unit source (sink) of flux; in addition, three units of flux all directed toward (away from) a "junction" can annihilate (be created) there. Such observations immediately lead to an understanding of the linear confinement potential of heavy quarkonia, to (approximately) linearly rising Regge trajectories, and to the idea that QCD is similar to the dual relativistic string theory of a decade ago.<sup>6</sup>

In the following we will extract our model from Hamiltonian lattice QCD, and then discuss in turn its general characteristics and its application to the simplest types of hadrons. Later we shall introduce some topics (multi-quark states, decay via flux-tube breaking, exotic-hadron phenomenology,...) which we are continuing to study, but concerning which we have some preliminary conclusions. In the final section of the paper we survey both what has been done and also the much larger body of work that remains to be done. A preliminary report on some of the results of this paper has been published elsewhere.<sup>7</sup> Some of the physical considerations presented in

arriving at our model from QCD are similar to those of Ref. 8. Its application to the simplest meson topology (see Sec. III A) is related to the work of Ref. 9.

## II. ORIGIN OF THE MODEL

### A. Hamiltonian lattice QCD

We begin the derivation of our model by reviewing Hamiltonian lattice QCD. As there are many excellent reviews available on the foundations of this subject,<sup>2</sup> we will mainly just quote those results which are important for our development.

In the Hamiltonian formulation of QCD on a cubic spatial lattice, the quark degrees of freedom “live” on the lattice sites while the gluonic degrees of freedom “live” on the links between these sites (see Fig. 1, where we also define some of our terminology). Let us consider first the theory without quarks: we describe this theory in terms of link variables  $U_l$  which (before quantization) are  $3 \times 3$  SU(3) group elements. The pure gauge-field Hamiltonian is then the sum of two parts, one involving only the  $U$ s and one which has nontrivial commutation relations with the  $U$ s:

$$H_{\text{glue}} = \frac{g^2}{2a} \sum_{\text{links } l} C_l^2 + \frac{1}{ag^2} \sum_{\text{plaquettes } p(l_1 l_2 l_3 l_4)} \text{Tr}[2 - (U_{l_4} U_{l_3} U_{l_2} U_{l_1} + \text{H.c.})] \quad (1)$$

with  $a$  the lattice spacing and  $g$  the corresponding coupling constant. Here  $C_l^2$  is defined in terms of the eight generators  $E_{l\pm}^a$  of SU(3) transformations of  $U_l$  at the beginning ( $-$ ) or the end ( $+$ ) of the link

$$[E_{l+}^a, U_l] = -\frac{\lambda^a}{2} U_l, \quad (2)$$

$$[E_{l-}^a, U_l] = +U_l \frac{\lambda^a}{2}, \quad (3)$$

by

$$C_l^2 = \sum_a (E_{l+}^a)^2 = \sum_a (E_{l-}^a)^2.$$

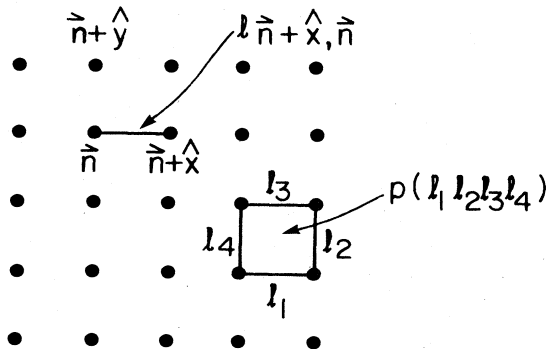


FIG. 1. A two-dimensional ( $x,y$ ) slice of the lattice showing a typical lattice point  $n = (n_x, n_y, n_z)$ , a typical link  $l_{n+\hat{x},n}$  from  $n$  to  $n+\hat{x}$ , and a typical plaquette  $p(l_1 l_2 l_3 l_4)$ .

In the second term the product of the  $U$ s is taken in order around the plaquette. To complete lattice QCD one simply adds to (1) a lattice Hamiltonian  $H_{\text{quark}}$  for the quarks interacting with the glue. With the quark fields as site variables we have

$$H_{\text{quark}} = \sum_{\text{flavors } q} m_q \sum_{\text{sites } n} q_n^\dagger q_n + \frac{1}{a} \sum_{\substack{\text{flavors } q \\ \text{links } l_{ji}}} q_j^\dagger U_{l_{ji}} \alpha_{l_{ji}} q_i, \quad (4)$$

where  $\alpha_{l_{ji}}$  is the Dirac matrix in the direction of the link  $l_{ji}$ .

Our complete Hamiltonian

$$H_{\text{QCD}}^{\text{lattice}} = H_{\text{glue}} + H_{\text{quark}}$$

has  $H_{\text{QCD}}$  in  $A^0=0$  gauge as its naive continuum limit; it is, furthermore, invariant under arbitrary time-independent gauge transformation at the lattice sites. Gauss' law takes the form of a constraint in the theory that the only physically relevant states are those which are gauge invariant. Finally, we mention that the quark Hamiltonian as written suffers from what is known as the “species-doubling problem,” but there are several methods for correcting this problem and this technical point need not concern us here.

In this formulation of QCD the lattice spacing  $a$  plays the role of the regulator mass in normal quantum field theory. Latticizing the theory also has another advantage: it allows one to set up a strong-coupling perturbation expansion in which the expansion parameter for lattice QCD is  $1/g$  instead of  $g$ . We may expect to be able to learn more about the strongly coupled regime of the theory in terms of such an expansion, and indeed this seems to be the case: for example, we will see below that confinement is an automatic property of the  $g \rightarrow \infty$  limit of lattice QCD. Moreover, the natural degrees of freedom of the strong-coupling regime are not quarks and gluons, but rather quarks and flux tubes, the latter being more in accord with various qualitative ideas on the nature of confinement in QCD. Of course, space is not coarse-grained (at least not on the scale of  $10^{-15}$  m), so that to relate lattice QCD to real QCD we must consider the limit  $a \rightarrow 0$ . In this limit,  $g \rightarrow 0$  so that a strong-coupling expansion must fail; this is just the other side of the failure of the weak-coupling expansion for small  $Q^2$ . Since, however, it can be shown that the two regimes “match” around  $g=1$ , thereby proving that lattice QCD as  $a \rightarrow 0$  is QCD, one nevertheless expects the strong-coupling expansion to be useful in many situations where large scales dominate, just as the weak-coupling expansion is useful for short-distance physics.

A simple analogy may be helpful. Consider approximating a continuous one-dimensional harmonic oscillator by a particle hopping along a one-dimensional lattice of points  $x = na$  ( $n = \dots, -2, -1, 0, 1, 2, \dots$ ) with lattice spacing  $a$ . The lattice Hamiltonian could be chosen to be

$$H_{mn} = \left[ \frac{1}{ma^2} + \frac{1}{2} ka^2 n^2 \right] \delta_{mn} - \frac{1}{2ma^2} (\delta_{m,n+1} + \delta_{m,n-1}) \quad (5)$$

since then the Schrödinger equation

$$i \frac{\partial \psi_m(t)}{\partial t} = H_{mn} \psi_n(t) \quad (6)$$

becomes

$$i \frac{\partial \psi(x,t)}{\partial t} = \left[ -\frac{1}{2m} \frac{\partial^2}{\partial x^2} + \frac{1}{2} kx^2 \right] \psi(x,t) \quad (7)$$

as  $a \rightarrow 0$ . Now for  $a \rightarrow \infty$  the potential-energy term  $\frac{1}{2}ka^2n^2\delta_{mn}$  dominates and the eigenstates correspond to the particle sitting on single lattice sites; corrections to this limit are of relative order  $\chi = 1/kma^4$  and one can proceed to systematically do perturbation theory in this hopping strength. Since the characteristic scale of the harmonic oscillator is  $\alpha^{-1} = (km)^{-1/4}$ , one will not get realistic wave functions or eigenenergies for the harmonic oscillator for  $a \gg \alpha^{-1}$  where lowest-order perturbation theory works well, but for  $\chi \sim 1$  one will begin to get good approximations to the solutions of the continuum problem if one works to sufficiently high order in  $\chi$ . By contrast, starting with free-particle solutions to the continuum Hamiltonian and treating  $\frac{1}{2}kx^2$  as a perturbation is hopeless. (The difference, of course, is that the hopping-parameter expansion for the ground state, for example, will be accurate if a matrix of dimension of order  $1/a\alpha$  is diagonalized.)

We are now ready to consider the properties of  $H_{\text{QCD}}^{\text{lattice}}$ . We note first that in the strong-coupling limit where  $a$  (and, as we shall see, therefore  $g$ ) is large, the only terms which survive are

$$H_{\text{SC}} = \frac{g^2}{2a} \sum_{\text{links}} C_l^2 + \sum_{q,n} m_q q_n^\dagger q_n. \quad (8)$$

The eigenvalues of  $C_l^2$  are just those of the square Casimir operator of SU(3): 0 for the singlet,  $\frac{4}{3}$  for 3 or  $\bar{3}$ ,  $\frac{10}{3}$  for 6 or  $\bar{6}$ , 3 for the octet, etc. The quark part of  $H_{\text{SC}}$  is, on the other hand, diagonalized by an arbitrary number of quarks and antiquarks at arbitrary lattice sites (subject to the exclusion principle). Since, however, the only physically relevant eigenstates are those which are gauge invariant, the strong-coupling eigenstates may be classified as follows.

(1) *The strong-coupled vacuum.* In this state all links are unoccupied ( $C_l^2 = 0$ ) and there are no fermions; the total energy  $E_{\text{vac}}$  is zero.

(2) *The pure glue sector.* There are still no quarks, but links are excited in such a way that gauge-invariant states are produced. The simplest such pure glue states ("glue loops") have a closed path of links in the 3 (or  $\bar{3}$ ) representation. These have energy  $(2g^2/3a^2)L$  where  $L$  is the length of the path; the simplest such state just has the links around the perimeter of an elementary plaquette excited:  $\text{Tr}(U_4 U_3 U_2 U_1) |0\rangle$  where  $|0\rangle$  is the vacuum. Of course more complicated configurations are allowed, including those with nontriple flux and those with more complicated topology<sup>10</sup> involving the three flux-link junctions in which the ends of three links are contracted at a single site with the invariant tensor  $\epsilon_{ijk}$ . See Fig. 2.

(3) *The meson sector.* The simplest quark-containing

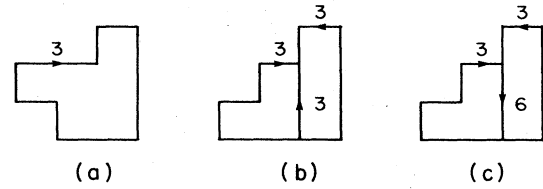


FIG. 2. Some pure glue states.

state consists of a quark and antiquark on the lattice joined by a path of flux links (for gauge invariance). These will have energy

$$m_q + m_{\bar{q}} + (2g^2/3a^2)L$$

so that we automatically have quark confinement in strong coupling. See Fig. 3.

(4) *The baryon sector.* The next simplest quark-containing state consists of three quarks connected by an  $\epsilon_{ijk}$ -type flux junction. Such quarks will also be confined. See Fig. 4.

(5) *Multiquark sectors.* When there are more quarks than those required for a meson or baryon, then in general the system will not be completely confined. The simplest such system consists of two quarks and two antiquarks. See Fig. 5.

With these examples, the general structure of the eigenstates of the strong-coupling limit is clear: it consists of "frozen" gauge-invariant configuration of quarks and flux lines. Of course these are not the eigenstates of QCD, but they do form a complete basis (in the limit  $a \rightarrow 0$ ) for the expansion of the true strong interaction eigenstates. Note that this clearly illustrates our earlier remark that there are more states in QCD than those possible in the quark model. Consider, for example, the "meson sector" defined above: in the quark model a meson is defined by the spins and relative coordinate of the quark and antiquark, but in QCD one must also specify the state of the flux between them.<sup>11</sup> We shall see later how these extra degrees of freedom imply the existence of hybrid mesons in QCD.

The full eigenstates of QCD can be found (in principle) by considering corrections to the strong-coupling limit from the terms we have neglected so far. These terms can induce a variety of effects. Consider first of all the  $(1/a)q^\dagger U a q$  term. It can, among other things, (1) annihilate a quark at one point and recreate it at a neighboring point with an appropriate flux link [Fig. 6(a)] and (2) break a three-flux line and create a quark-antiquark pair [Fig. 6(b)]. This term thus plays a role analogous to both the quark kinetic-energy term and the quark-gluon coupling term of the weak coupled theory. Next consider the

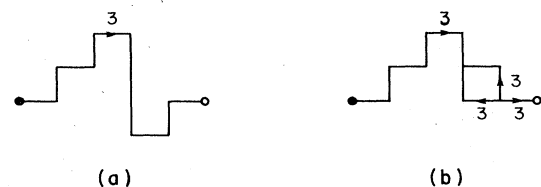


FIG. 3. Some meson states.

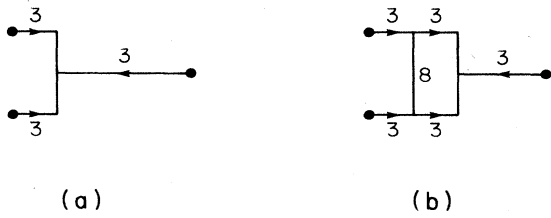


FIG. 4. Some baryon states.

$$\frac{1}{ag^2} \text{Tr}[2 - (U_{l_4} U_{l_3} U_{l_2} U_{l_1} + \text{H.c.})]$$

term. It can, among other things (1) allow flux to hop across plaquettes [Fig. 7(a)] and (2) change flux topology [Fig. 7(b)].

We now consider an instructive calculation on the departures from the strong-coupling limit: we will examine the effects of such departures on quark confinement by considering two infinitely massive quarks separated by  $N$  lattice sites along an axis of the lattice. In the strong-coupled limit, ignoring the constant  $2m_Q$ ,

$$E_{Q\bar{Q}} - E_{\text{vac}} = \frac{2g^2}{3a^2} L = \frac{2g^2}{3a^2} Na. \quad (9)$$

Since we wish to associate this energy with the linear potential  $bL$  of quark models (to be discussed below), we would require that  $2g^2/3a^2 = b$ . This in turn shows that the bare coupling  $g$  must be chosen to depend on  $a$ :  $g^2(a) = (3/2)ba^2$ , and we see already that as we let  $a$  decrease so that we can recover the continuum limit, we will eventually encounter values of  $g$  that require consideration of corrections to the strong-coupling limit. In the case at hand the lowest-order corrections will consist of (1) corrections to  $E_{\text{vac}}$  via mixing between the strong-coupled vacuum and states with single excited plaquettes and (2) corrections to  $E_{Q\bar{Q}}$  via mixing between the straight line of flux and flux configurations with (a) kinks, (b) connected loops of flux, and (c) disconnected excited plaquettes [Figs. 8(a), 8(b), and 8(c)].

The result of such a second-order calculation is that

$$E_{Q\bar{Q}}^{(2)} - E_{\text{vac}}^{(2)} = \frac{2g^2}{3a^2} L \left[ 1 - \frac{11\chi^2}{204} \right], \quad (10)$$

where  $\chi = 2/g^4$  is the strong-coupling expansion parameter. We see that we still have a linear confinement potential with

$$b^{(2)} = \frac{2g^2}{3a^2} \left[ 1 - \frac{11}{51g^8} \right]. \quad (11)$$

Note that to maintain the same physical string tension we

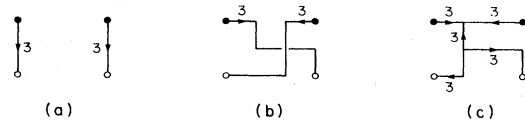


FIG. 5. Some  $qq\bar{q}\bar{q}$  states

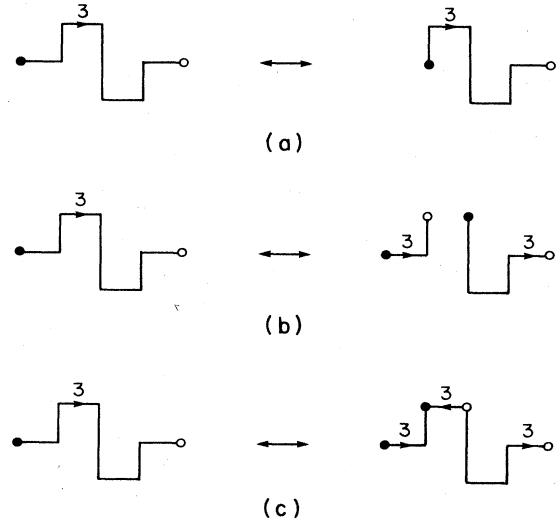


FIG. 6. (a) Quark hopping. (b) Flux-breaking pair creation. (c)  $q\bar{q}$  "seeding."

must now choose

$$g^2(a) = \frac{3}{2}ba^2 \left[ 1 + \frac{176}{4131b^4a^8} \right]. \quad (12)$$

Clearly this calculation can be carried out in principle to arbitrarily high order.<sup>12</sup> When one does this one will find

$$b = \frac{1}{a^2} f(g^2), \quad (13)$$

where  $f(g^2)$  is a pure power-series expansion in  $1/g^2$ . If

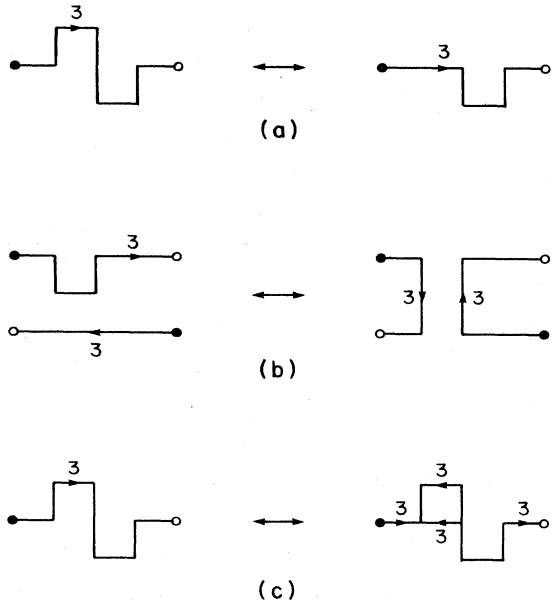


FIG. 7. (a) Flux-tube hopping. (b) Flux-tube topological mixing by rearrangement. (c) Flux-tube topological mixing by "bubble formation."

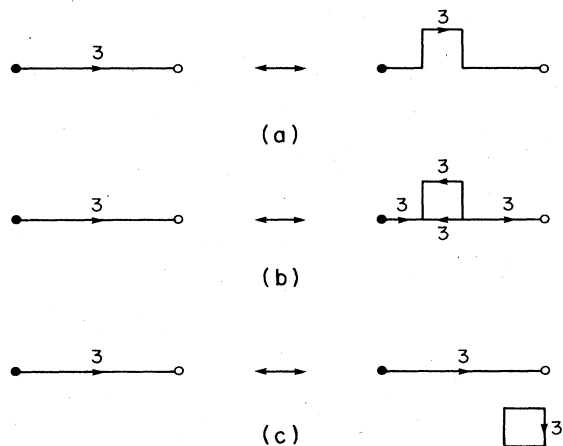


FIG. 8. Some lowest-order corrections to the  $Q\bar{Q}$  ground state.

QCD is to confine then we see that as  $a \rightarrow 0$  we must be able to choose  $g(a)$  in such a way that  $b$  remains fixed at its physical value. This requirement, along with the requirement that, as  $a \rightarrow 0$ ,  $g(a)$  must behave as deduced from weak coupling, shows that confinement, while natural, is not trivial in lattice QCD. Incidentally, from the fact that  $db/da=0$  and from knowledge of  $g(a)$  from weak coupling, one can deduce that as  $a \rightarrow 0$

$$f(g^2) = \frac{b}{\Lambda^2} (\beta_0 g^2)^{-\beta_1/\beta_0^2} \exp(-1/\beta_0 g^2), \quad (14)$$

where  $\Lambda$  is a constant, and where  $\beta_0 = 11/16\pi^2$  and  $\beta_1 = 102/256\pi^4$  are the first two coefficients in the expansion of the perturbative “ $\beta$  function” of asymptotic-freedom fame. Note that  $f(g^2)$  has no power series expansion near  $g^2=0$ , proving that confinement cannot be seen in QCD via perturbation theory about weak coupling. This clearly makes the strong-coupling expansion the more attractive starting point for understanding hadron physics.

### B. The flux-tube model for QCD

We are now in a position to give a first general definition of our model. As already stressed, although the strong-coupling eigenstates are not the eigenstates of QCD, they are a complete basis for QCD. Thus if we could diagonalize  $H_{\text{QCD}}^{\text{lattice}}$  in this basis for sufficiently small lattice spacing  $a$ , we would be able to solve the theory. We propose that it is useful to reorganize the Hamiltonian matrix into blocks of a given topology<sup>10</sup> and then to diagonalize within each block, before taking into account interblock mixing. In other words, we first treat quark hopping and flux-tube oscillation exactly and then consider the mixing between such topological blocks. This corresponds to a generalization of the type of Fock-space expansion that has proved useful in the quark model: it seems to be a reasonable first approximation (for low-lying states at least) to neglect meson widths which correspond to a mixing between the  $q\bar{q}$  and  $qq\bar{q}\bar{q}$  sectors of the theory. We hope to treat not only this as-

pect of the  $(1/a)q^\dagger U a q$  term as a perturbation, but also all other nontopologically diagonal departures from the strong-coupling limit. Of course the utility of this program is dubious for processes that are dominated by the (weak) perturbative regime of QCD. We shall deal with this issue below; we do not think this is an impediment to the successful treatment of hadronic objects which are in all presently known cases dominated by the nonperturbative regime.

To illustrate the model in more detail in a simple context, consider first a heavy  $Q\bar{Q}$  pair and ignore all pair creation effects. Then the strong-coupled basis states for this system will consist of all possible flux-tube topologies which are consistent with Gauss’ law, including a single flux tube flowing from  $Q$  to  $\bar{Q}$  via an arbitrary path in the lattice, various branching flux tube shapes, and configurations with disconnected flux excitations. As our first approximation we consider only those departures from strong coupling which “unfreeze” the quarks and flux tubes into objects with kinetic energy, but ignore mixing between these topological sectors. The transition between frozen and fluid flux tubes corresponds to the “roughening transition”<sup>13</sup> seen in numerical lattice work and clearly corresponds to an essential requirement for relating any lattice calculation to continuum physics (compare to the harmonic-oscillator example of the previous section). In the case where the  $Q\bar{Q}$  separation  $r$  is large, we can expect to approximate the state of the system in terms of a lattice of scale  $a$  with  $r \gg a \sim \lambda_0$  where  $\lambda_0 \sim b^{-1/2}$  is the scale where  $g \sim 1$  and topological mixing becomes important. With such a lattice, interblock mixing will be weak and our model will describe this system in terms of a (perturbed) discrete string. For infinitely heavy quarks with separation  $r \gg \lambda_0$ , the ground state of this system will be well approximated by a  $Q\bar{Q}$  pair with a string in its quantum-mechanical ground state, the first excited state will be doubly degenerate with either a right- or left-handed phonon excited in the lowest string mode, etc. As the distance  $r$  is slowly varied, the eigenenergy of the string eigenstate  $S$  will trace out an adiabatic potential  $V^S(r)$ , and we will associate such potentials with an adiabatic approximation to the physics of mesons. When the  $Q\bar{Q}$  pair move in the adiabatic potential  $br$  of the ground state of this QCD quantum string, one recovers the usual spectrum of mesons in the quark model. When the pair moves in the adiabatic potential of an excited string, the resulting hadrons correspond to a new species not contained in the usual quark model: hybrid mesons with both quark and gluonic degrees of freedom in evidence.

The baryon sector, while more complicated, is analogous to the mesons: the ordinary baryons of the quark model correspond to three quarks moving in the adiabatic potential of the ground state of the three-junction ( $Y$ ) string, while excited strings will lead to hybrid baryons. The phenomenology of hybrid mesons and baryons will be discussed in a later section.

Even more novel than the hybrid states are those made of pure glue, which correspond in the model, in the same approximation, to the various quantum states of a closed loop of (discrete) string. The phenomenology of such states will also be discussed below.

In multi-quark systems we are for the first time forced to go beyond the simple vibrating-string picture to consider an essential role for topological mixing. This is because in such systems adiabatic surfaces will always cross in the absence of mixing, as can be seen by considering Fig. 7(b) for the case when the  $qq\bar{q}\bar{q}$  system is arranged at the corners of a square. Such systems are consequently considerably more complicated than those we have already considered.

Of course the simple classification scheme we have presented here is both incomplete and inaccurate. For example, one must expect to find (at high masses) "topological meson hybrids" in which the  $Q\bar{Q}$  system moves in the potential of more complicated string topologies. There will, in addition to mixing between topologies via the

$$\frac{1}{ag^2} \text{Tr}[2 - (U_{l_4} U_{l_3} U_{l_2} U_{l_1} + \text{H.c.})]$$

term, be deviations from the adiabatic limit that mix states with different phonon excitations. While all such effects can be described within the context of this model, its utility will depend on the degree to which they are weak at least for low-lying states. Perhaps the very success of the naive quark model for mesons and baryons provides some evidence in favor of the viability of such a separation.

Although we have argued for the validity of this approximation for large-scale phenomena in QCD, it must fail at short distances where  $g \rightarrow 0$ . As  $a \rightarrow 0$ , mixing will become increasingly strong and the state of the gluonic degrees of freedom in our  $Q\bar{Q}$  example will become an increasingly complicated mixture of flux-tube topologies. This is to be expected: in this regime QCD is most simply described in terms of quarks with a weakly coupled octet of vector gluons, and we know that the linear potential must be modified. We will more fully discuss this difficult interface between strong and weak coupling in the context of the systems we will encounter below.

With this general survey of the model completed, we are ready to apply it to various specific systems. We will return in the final sections to consequences of the model which could be checked with numerical lattice simulations and to generalizations of the model to other gauge theories.

### III. HADRONS IN THE FLUX-TUBE MODEL

In this section we will present the results of a first, rough survey of the consequences of the flux-tube model for hadrons. It will become apparent from the development which ensues that a more precise discussion will require the inclusion of a number of "second-order" effects (which are presently under study and on which we expect to report in due course), but we believe this survey should adequately portray the main features of the terrain.

#### A. Mesons and meson vibrational hybrids

We first consider again a system consisting of static quark and antiquark sources a large distance  $r \gg b^{-1/2}$  apart. As we have already argued, in this case the system will behave like a quark and antiquark connected by a discretized quantum string. The lowest excitations of such a string will correspond to nonrelativistic, small

transverse displacement oscillations and so should be well described by the Hamiltonian of a continuous string

$$H_S = b_0 r + \frac{1}{b_0 r} \sum_m \sum_{i=1}^2 (\pi_m^i \pi_m^i + \frac{1}{4} \omega_m^2 b_0^2 r^2 q_m^i q_m^i), \quad (15)$$

where  $q_m^i$  and  $\pi_m^i$  are string normal coordinates and their conjugate momenta defined in terms of the transverse string displacement vector  $\mathbf{y}(\xi)$  with  $0 \leq \xi \leq 1$  by

$$\mathbf{y}(\xi) = \sum_{i,m} \hat{\mathbf{e}}_i q_m^i y_m(\xi), \quad (16)$$

where  $y_m(\xi)$  is the  $m$ th normal mode,  $\hat{\mathbf{e}}_i$  ( $i=1,2$ ) are unit vectors orthogonal to the interquark separation  $\mathbf{r} = \mathbf{r}_q - \mathbf{r}_{\bar{q}}$ , and  $\xi r$  is the distance along the undisplaced string of the displacement  $\mathbf{y}(\xi)$ . In the harmonic approximation appropriate to the low-lying excitations, one would have simply

$$y_m(\xi) = \sin m \pi \xi, \quad (17)$$

$$\omega_m = \frac{m \pi}{r}. \quad (18)$$

It should be noted that the "bare" string tension  $b_0$  appearing in (15) should not be identified with the physical string tension  $b$  which, as we will see immediately, includes effects arising from the zero-point energy of the string.

The quantization of (15) for fixed  $\mathbf{r}$  is of course straightforward: the eigenstates are characterized by phonon occupation numbers  $n_m^i$  with the phonons labeled by their mode  $m$  and polarization  $i$ ; the eigenenergies are accordingly

$$E(n_m^i) = b_0 r + \sum_{m,i} (n_m^i + \frac{1}{2}) \omega_m. \quad (19)$$

For most purposes the continuum approximation (15) to our string is adequate, but to discuss its zero-point energy, we must recall that the string should be considered to be discrete on a scale  $a$ . The modifications required to effect this discretization are minimal: in (15) replace  $\sum_m$  by  $\sum_{m=1}^N$  where  $(N+1)a = r$ , recognize that  $\xi$  should take on the discrete values  $na/r$  ( $n=0, \dots, N+1$ ), and in the harmonic approximation take

$$y_m(n) = \sin \left[ \frac{m \pi n}{N+1} \right], \quad (20)$$

$$\omega_m = \frac{2}{a} \sin \frac{m \pi}{2(N+1)} \quad (1 \leq m \leq N). \quad (21)$$

The zero-point energy can be evaluated exactly in this approximation to give

$$E_0 - b_0 r = \sum_{m=1}^N \sum_{i=1}^2 \frac{1}{2} \omega_m = \frac{\sqrt{2}}{a} \left[ \frac{\sin[\pi N/4(N+1)]}{\sin[\pi/4(N+1)]} \right] \quad (22)$$

$$\simeq \left[ \frac{4}{\pi a^2} \right] r - \frac{1}{a} - \frac{\pi}{12r} + \dots \quad (23)$$

We see explicitly in this example that the zero-point energy contributes to the physical string tension, and also that it produces a constant term, a Coulomb-type term, and so on.

We believe that one must interpret these terms with some care: it is important to realize that the relevant quantity is not the absolute energy of the system we are considering, but rather its energy relative to the vacuum. In this regard, recall that the structure of the vacuum will be modified from that of the strong-coupling vacuum at the small scale  $\lambda_0 \sim b^{-1/2}$  by vacuum fluctuations. Although these fluctuations are strictly speaking the effects of mixing between topologically distinct sectors of the theory and should not therefore logically be considered at this stage, their existence will have an effect on the energy of the static  $Q\bar{Q}$  system which we are considering. It follows that (23) is incomplete: the presence of the string will modify these fluctuations and therefore affect  $E_{Q\bar{Q}} - E_{\text{vac}}$  (see Sec. IIA for an explicit example). We should not be surprised that we are unable to calculate the physical string tension: this is analogous to the situation in QCD where the physical string tension sets the scale of the whole theory and where it (or some substitute for it like  $\Lambda_{\text{QCD}}$ ) must be used as input to the renormalization program. In contrast, the constant term in (23) is in principle calculable from QCD, but here we are forced to introduce such a constant term  $c$  as a parameter which we can only constrain very roughly to have the order of magnitude  $b^{1/2}$ . Finally, we consider the  $-\pi/12r$  term which has some celebrity since, unlike any of the other terms in (23) (including those omitted), its precise coefficient  $-\pi/12$  has been shown to have a very general validity.<sup>8</sup> From our point of view, however, the existence of this term is rather irrelevant. It is, to be sure, the term which arises from the zero-point motion of our stringlike degrees of freedom, but topological mixing effects, which produce departures from the "thin-string" approximation, will modify this idealized behavior. Indeed we know that the sum of all such effects must produce a transition from a gluon field with energy  $br$  at large distances to a ground state of the gluon field with energy  $-4\alpha_s(r)/3r$  at distances  $r < b^{-1/2}$ . It is thus natural to assume the usual two-component Coulomb + linear model for the ground-state energy of the gluon fields in this situation

$$E^0(r) = -\frac{4\alpha_s(r)}{3r} + c + br \quad (24)$$

and to presume that the transition region will be smoothly interpolated by this model.

We can now continue to consider further consequences of (15). In the presence of static sources we see that the gluon field has a *sequence* of states  $S$  with energy levels characterized by the phonon mode occupation numbers  $n_m^i$ . As a first approximation, valid in the limit of heavy quarks, we will treat these eigenenergies  $E^S(r)$  associated with the string states  $S$  as adiabatic potentials in which the quarks move.

The ordinary mesons of the quark model thus correspond to a quark and antiquark moving in the adiabatic potential (24) corresponding to the ground-state eigenener-

gy  $E^0(r)$  of the gluon field. From this point of view we can see that the quark model should work in conditions where it treats states of quarks moving in this lowest adiabatic potential which are well separated in energy, on a scale set by the quark oscillation frequencies, from the next (excited gluon state) adiabatic potential of the same quantum numbers. The flux-tube model thus automatically recovers the quark model for heavy-quark spectroscopy and tells us how to systematically correct the quark model in situations where there are violations of its conditions of validity.<sup>14</sup>

The flux-tube model also gives us new kinds of mesons, the simplest being the "vibrational hybrids" which, in the adiabatic limit, correspond to a quark and antiquark moving in an excited string adiabatic potential  $E^S(r)$  for  $S \neq 0$ . We will devote most of the remainder of this subsection to the derivation of the masses and quantum numbers of the lowest-lying such states.

Consider the lowest hybrid adiabatic potential with one  $m=1$  phonon. We expect the appropriate adiabatic potential  $E^1(r)$  to be modified from  $E^0(r)$  in two ways: it will include a term  $+\pi/r$  from exciting the phonon, and at small  $r$  the Coulomb term  $-4\alpha_s/3r$  appearing in  $E^0(r)$  will be replaced by the appropriate short-distance gluon-field energy which evolves adiabatically from the excited string. (Very roughly speaking, at short distances these states will display a gluonic field with a local excitation but clearly this excitation need not be closely related to a weak-coupling gluon.) As  $r \rightarrow 0$  the  $q$  and  $\bar{q}$  will lie on top of one another, but the excitation in the gluon field, which will carry the memory of its adiabatic ancestry explicitly in its quantum numbers, will have an extension  $b^{-1/2}$ . It is thus natural to assume that as  $r \rightarrow 0$  the  $\pi/r$  does not blow up, but rather evolves to some fixed finite value of order  $\pi b^{1/2}$ . We therefore take

$$E^1(r) = -\frac{4\alpha_s}{3r} + c + br + \frac{\pi}{r}(1 - e^{-fb^{1/2}r}) \quad (25)$$

with  $f$  a number of order unity. Fortunately, as we shall see, our results will not be very sensitive to this short-distance cutoff parameter  $f$ . (Our original results<sup>7</sup> were for  $f = \infty$ .)

We are now ready to discuss the meson and meson vibrational hybrid spectra and quantum numbers in a very rough fashion. For the ordinary mesons we use the effective quark Schrödinger equation

$$H^0 = -\frac{1}{2\mu} \frac{\partial^2}{\partial r^2} + \frac{L(L+1)}{2\mu r^2} + E^0(r), \quad (26)$$

where  $\mu$  is the  $q\bar{q}$  reduced mass. Taking the standard string tension  $b=0.18 \text{ GeV}^2$ , the constituent quark masses  $m_u = m_d = 0.33 \text{ GeV}$ ,  $m_s = 0.55 \text{ GeV}$ ,  $m_c = 1.77 \text{ GeV}$ , and  $m_b = 5.17 \text{ GeV}$ , the constant  $c = -0.7 \text{ GeV}$ , and taking a mean value of

$$\frac{4\alpha_s}{3} \simeq \begin{cases} 1.1 & \text{for } u, d, s \text{ mesons,} \\ 0.5 & \text{for } c\bar{c} \text{ and } b\bar{b} \end{cases}, \quad (27)$$

then gives a reasonable picture of the gross level structure (before spin-dependent interactions) of ordinary meson spectroscopy. This procedure thus sets all of our parameters except  $f$ .

Now consider the mesons which live on  $E^1(r)$ . There are two transverse polarization states of the string, which may be taken to be clockwise and anticlockwise about the quark-antiquark axis. In general if  $n_{m+}$  ( $n_{m-}$ ) is the number of clockwise (anticlockwise) phonons in the  $m$ th mode and  $\Lambda = \sum_m (n_{m+} - n_{m-})$ , the dependence of the string wave function on the angle  $\gamma$  about the axis is  $e^{i\Lambda\gamma}$ . The quantity  $\Lambda$  is therefore the angular momentum component about this axis. Since clockwise and anticlockwise polarizations interchange under the parity operation, the states for nonzero  $\Lambda$  will occur in parity doublets. This parity doubling is a well-known property of the adiabatic limit for systems which have the symmetry of a symmetric rotator. As shown in the Appendix, for such a system the quark angular wave function for orbital angular momentum  $L$  and axial component  $M$  is  $D_{M\Lambda}^L(\phi, \theta, -\phi)$  and the centrifugal barrier, ignoring transitions between adiabatic surfaces, is

$$\frac{1}{2\mu r^2} \langle \mathbf{L}_q^2 \rangle = \frac{L(L+1) - \Lambda^2 + \langle \mathbf{L}_{S_1}^2 \rangle}{2\mu r^2}. \quad (28)$$

Here  $\mathbf{L}_q$  is the quark angular momentum operator and the two components of  $\mathbf{L}_{S_1}$  are the raising and lowering operators of the angular momentum component along the axis. We drop the last term in (28). Its effect is to raise somewhat the lowest hybrid masses<sup>14</sup> (see also Sec. V A). Using the effective radial Hamiltonian for the first hybrid surface

$$H^1 = -\frac{1}{2\mu} \frac{\partial^2}{\partial r^2} + \frac{L(L+1) - \Lambda^2}{2\mu r^2} + E^1(r) \quad (29)$$

we get the predictions for hybrid masses listed in Table I. The quantum-number assignments shown in Table I are also derived in the Appendix.

We stress that the mass estimates of Table I are rather crude: we would estimate their reliability to be no better than  $\pm 100$  MeV for the center of gravity of each flavor sector. In addition we recall that in this same approximation the  $A_2(1320)$ ,  $B(1235)$ , and  $A_1(1250)$  are all degenerate: we have not considered here the question of spin-

dependent perturbations. Some may consider our neglect of these relativistic corrections less serious than our use of the Schrödinger equation to describe the quark motion and the use of the small oscillation, nonrelativistic approximation for the string motion in the first place. Indeed, we agree that relativistic effects are very important, especially in the light mesons and for short strings, but we believe that a large fraction of these effects can be successfully subsumed into the choice of the parameters of a nonrelativistic model.

We reserve a discussion of the phenomenology of these states to Sec. VI.

### B. A nonrelativistic model of glue loops

The pure glue sector of the model appears in principle to be simpler than the meson sector just discussed. However, the absence of the static quark limit means that there is no natural adiabatic limit such as that used for mesons. It nevertheless seems reasonable to suppose that the simplest topology, the single loop of flux, will form the basis of the lowest-lying states. We describe position on this torus of flux by the cylindrical coordinates  $(z, \rho, \Phi)$  where  $+\hat{z}$  defines the orientation of the loop's arrow by the right-hand rule. Expanding about a circular loop of flux with  $z=0$  and mean radius  $\rho_0$  we then have

$$\rho(\Phi) = \hat{\rho} \left[ \rho_0 + \sum_{m=2} (\alpha_m^{\rho} \sin m\Phi + \beta_m^{\rho} \cos m\Phi) \right] + \hat{z} \sum_{m=2} (\alpha_m^z \sin m\Phi + \beta_m^z \cos m\Phi) \quad (30)$$

and we treat  $\rho_0$  and the Fourier-expansion coefficients  $\alpha_m^{\rho}, \beta_m^{\rho}, \alpha_m^z, \beta_m^z$  as quantum variables. The Fourier sum starts at  $m=2$  since the  $m=1$  modes correspond to pure translation and rotation. In addition to these variables the system (in its rest frame) requires two further variables  $(\theta, \phi)$  to specify the orientation of the (body-fixed)  $\hat{z}$  axis in space.

We now assume that the motion in  $(\rho_0, \theta, \phi)$  may be treated by the adiabatic approximation in the same way as was the motion in  $(r, \theta, \phi)$  for the meson string in the previous section. For fixed  $(\rho_0, \theta, \phi)$  the Hamiltonian of the closed string is

TABLE I. Some low-lying meson hybrids.

Flavor	$J^{PC}$ or $J^P$	Mass (GeV) for $f=1$	$\frac{dm}{df}$ (GeV)	$\Delta m^a$ (GeV)	$m^b$ (GeV)
$I=1$	$2^{\pm\mp}, 1^{\pm\mp}, 0^{\pm\mp}, 1^{\pm\pm}$	1.67	0.08	0.19	$\sim 1.9$
$I=\frac{1}{2}$	$2^{\pm}, 1^{\pm}, 0^{\pm}, 1^{\pm}$	1.80	0.10	0.17	$\sim 2.0$
$I=0$ $\left[ \frac{u\bar{u} + d\bar{d}}{\sqrt{2}} \right]$	$2^{\pm\mp}, 1^{\pm\mp}, 0^{\pm\mp}, 1^{\pm\pm}$	1.67	0.08	0.19	$\sim 1.9$
$I=0$ ( $s\bar{s}$ )	$2^{\pm\mp}, 1^{\pm\mp}, 0^{\pm\mp}, 1^{\pm\pm}$	1.91	0.12	0.14	$\sim 2.1$
$c\bar{c}$	$2^{\pm\mp}, 1^{\pm\mp}, 0^{\pm\mp}, 1^{\pm\pm}$	4.19	0.18	0.06	$\sim 4.3$
$b\bar{b}$	$2^{\pm\mp}, 1^{\pm\mp}, 0^{\pm\mp}, 1^{\pm\pm}$	10.79	0.28	0.02	$\sim 10.8$

<sup>a</sup>Contribution to the mass from nonadiabatic effects, taken from Ref. 14.

<sup>b</sup>A "best guess" based on the previous columns.

$$H_S = 2\pi b_0 \rho_0 + \sum_{i,m} \left[ \frac{\pi_i^2}{2\pi b_0 \rho_0} + \frac{m^2 \pi b_0}{2\rho_0} \gamma_i^2 \right], \quad (31)$$

where  $\gamma_i$  are the normal coordinates  $\alpha_m^p, \beta_m^p, \alpha_m^z, \beta_m^z$  for each  $m$  and the  $\pi_i$  are their conjugate momenta. If as in Sec. III A we apply a short-wavelength cutoff by discretizing the string at a scale  $a \sim \lambda_0$ , then we get a ground-state zero-point energy  $\mathcal{E}_0$  as a function of the mean circumference  $\mathcal{C} = 2\pi\rho_0$  of the glue loop given by

$$\mathcal{E}_0 - b_0 \mathcal{C} \simeq \left[ \frac{4}{\pi a^2} \right] \mathcal{C} - \frac{13\pi}{3\mathcal{C}} + \dots \quad (32)$$

to be compared with (23). For a large loop the excluded small-scale vacuum fluctuations per unit length should be the same as for a long straight flux tube; it therefore seems clear, since the coefficient of  $\mathcal{C}$  in (32) and  $r$  in (23) are identical, that the “renormalized” string tension in this case should as in mesons be  $b$ . The absence of a constant term in (32) is cutoff dependent and in any event, in view of the effect of the loop on vacuum fluctuations, we must expect that there will be a constant  $c'$  associated with the glue-loop zero-point energy. The Coulomb-type  $-13\pi/3\mathcal{C}$  term is, like the  $-\pi/12r$  term in mesons, cutoff independent. However, as in that case we would argue that the effects of topological mixing at small scales make this fact irrelevant. For mesons we could argue that the lowest-lying adiabatic potential should connect smoothly onto  $-4\alpha_s/3r$ , but unfortunately here we have no such limit to guide us. We must therefore allow for a generic effective potential in this case of the form

$$\mathcal{E}^0(\rho) = 2\pi\rho b + c' - \frac{\gamma}{\rho} (1 - e^{-f'b^{1/2}\rho}) \quad (33)$$

and are forced to accept the fact that we will be unable to predict the ground-state glue-loop mass with precision. In addition to its ground state, (31) has vibrationally excited states, the lowest of which are four degenerate  $m=2$  states with excitation energy  $2/\rho$  which have  $\Lambda=2$  about the  $\hat{z}$  axis; we expect for these states an energy

$$\mathcal{E}^2(\rho) = 2\pi\rho b + c' + \frac{2-\gamma}{\rho} (1 - e^{-f'b^{1/2}\rho}). \quad (34)$$

In Eqs. (33) and (34), we have introduced a parameter  $f'$  to play a similar role to the parameter  $f$  we introduced for the hybrid states. In the adiabatic approximation in  $(\rho_0, \theta, \phi)$  each eigenstate of  $H_S$  will yield such a potential surface for an effective Schrödinger equation in the variable  $\rho$ . Changing to the variable  $\xi = \rho^{3/2}$  this takes the form

$$\left[ -\frac{d^2}{d\xi^2} + \frac{J(J+1) - \Lambda^2}{2\pi\xi^2} + \mathcal{E}^N(\xi^{2/3}) \right] \psi(\xi) = E\psi(\xi) \quad (35)$$

with the boundary condition that  $\psi(0)=0$ . The spectrum is quite complex. It consists of the following states.

(1) The ground-state “breathing mode” and its radial excitations with  $J^{PC}=0^{++}$ .

(2) A set of orbitally excited states with  $J^{PC}=1^{+-}, 2^{++}, 3^{+-}, \dots$  built on each  $0^{++}$  “breathing mode” state.

(3) A further set of two parity doublets of opposite  $C$  with  $\Lambda=2, J=2$  each with their radial and orbital excitations.

(4) A set of states with two  $m=2$  phonons with  $\Lambda=0$  and  $J=0$  which are low-lying since they avoid the centrifugal-barrier effect in (35).

(5) Many further states at higher mass.

Table II gives a summary of the lowest glue-loop quantum numbers and masses. Note, incidentally, that the lowest  $0^{-+}$  state lies more than 1 GeV above the ground state.

### C. Baryons and baryon vibrational hybrids

The baryons of the usual quark model correspond in this picture to three quarks moving in the adiabatic potential generated by the ground-state energy  $\epsilon_0(\mathbf{r}_1, \mathbf{r}_2, \mathbf{r}_3)$  of the three flux-tube junction tying together quarks at positions  $\mathbf{r}_1, \mathbf{r}_2$ , and  $\mathbf{r}_3$ ; excitations of the normal modes of this flux tube configuration correspond to baryon vibra-

TABLE II. Some low-lying pure glue states. The similar masses given in Ref. 7 were for the values  $c'=c, \gamma=0$ , and  $f'=\infty$ . As discussed in the text, the true values of these parameters are unknown; the values chosen for the masses given here are only suggestive. Note that splittings are relatively insensitive to this choice, but in general absolute masses are not. The exceptions to this comment on the stability of splittings are the four degenerate  $J=2$  vibrational states which have moved down by 0.4 GeV and the four degenerate  $J=0$  states (not mentioned in Ref. 7) which would be considerably higher in mass with  $f'=\infty$ .

$J^{PC}$	Mass (GeV) for		$\frac{dm}{dc'}$	$\frac{dm}{d\gamma}$ (GeV)	$\frac{dm}{df'}$ (GeV)
	$c'=0, \gamma=\frac{13}{6}, f'=1$				
$0^{++}$	1.52	1	-0.32	-0.18 $\gamma$	
$1^{+-}$	2.25	1	-0.29	-0.13 $\gamma$	
$0^{++}$	2.75	1	-0.28	-0.12 $\gamma$	
$0^{++}, 0^{+-}, 0^{-+}, 0^{--}$	2.79	1	-0.31	+ 0.17(4- $\gamma$ )	
$2^{++}$	2.84	1	-0.27	-0.11 $\gamma$	
$2^{++}, 2^{+-}, 2^{-+}, 2^{--}$	2.84	1	-0.29	+ 0.13(2- $\gamma$ )	
$1^{+-}$	3.25	1	-0.27	-0.11 $\gamma$	
$3^{+-}$	3.35	1	-0.26	-0.09 $\gamma$	

tional hybrids.

The quantization of these flux-tube degrees of freedom would obviously be a formidable task, and we have not yet attempted it. We nevertheless believe that there are some useful observations which can be made, based on the fact that when two of the quarks in a baryon are close to one another, the flux-tube structure of the system will resemble that of a meson so that its energy should be the meson energy in that limit. If we make the simple assumption that the linear part of  $\epsilon_0$  should depend only on the minimum string length  $l(\mathbf{r}_1, \mathbf{r}_2, \mathbf{r}_3)$  defined by  $\mathbf{r}_1$ ,  $\mathbf{r}_2$ , and  $\mathbf{r}_3$ , then it must have the form

$$\epsilon_0 = bl + c_3 + \dots, \quad (36)$$

where  $c_3$  may differ from  $c$  since this constant term will in general depend on the number of string ends, but where  $b$  is the same as in mesons since in the limit  $\mathbf{r}_1 = \mathbf{r}_2$ ,  $l$  would play the role of  $r$  in mesons. If we make the usual condition that at short distances  $\epsilon^0$  must match the one-gluon-exchange potential, then we have

$$\epsilon^0(\mathbf{r}_1, \mathbf{r}_2, \mathbf{r}_3) = bl(\mathbf{r}_1, \mathbf{r}_2, \mathbf{r}_3) + c_3 - \sum_{i < j} \frac{2\alpha_s(r_{ij})}{3r_{ij}}. \quad (37)$$

We note that the constant term may differ from what one would have expected if the baryon effective potential were a sum of two body potentials each with half the meson strength, though the Coulomb term has this property and the linear term has it as an approximation.

Studies of three quarks moving in a potential such as this have shown that it can give a reasonable description of the spin-independent spectrum of baryons,<sup>15</sup> and it is reasonable to expect that when supplemented with some spin-dependent interactions this picture will reproduce the successful phenomenology of more naive models. Therein lies a certain danger, however, since our present understanding of baryon phenomenology makes it very difficult to accommodate any further states below about 2 GeV, where one might have expected baryon hybrids. We consider it one of the successes of our model that, in contrast to other models for hybrids, one here expects the lowest-lying hybrids to appear only above 2 GeV. That this is so can be seen from the meson-baryon connection discussed above and the fact that the corresponding gap in mesons is around 1.3 GeV, while the spin-averaged ground-state  $S=0$  baryons are at 1.1 GeV.

On the basis of such an estimate we expect the lowest-lying baryon vibrational hybrids to be SU(6) 70-plets with their spin-averaged strangeness  $S$  members at about 2.4 GeV  $+ \frac{1}{3} |S| (M_{\Omega^-} - M_{\Delta})$ . Since baryons cannot have exotic quantum numbers, it may be rather difficult to disentangle such states from the very rich spectrum of ordinary baryons at these masses.

#### D. Topological hybrids

We have consistently assumed in the preceding sections that the lowest-lying hybrid mesons, hybrid baryons, and excited pure glue states would have the character of vibrating strings or loops of string. However, at some energy we must expect to encounter, for example, hybrid

mesons in which the quark and antiquark move in the effective potential generated by more complex flux-tube topologies. We have, as might be imagined, not quantized such string configurations, but we observe that each new loop introduced into the simplest topology will generate not only an extra length of flux tube but also two junction points each of which has a longitudinal degree of freedom. If the hadron in question is characterized by a size  $\delta$ , then a topology with  $\lambda$  extra loops will have on the order of an extra length  $\lambda\delta$  of flux tube and the zero-point motion of  $2\lambda$  junctions each constrained to a distance of order  $\frac{1}{2}\delta$ . This will give an extra energy of order  $\lambda\delta b + 4\lambda/\delta$  which is always greater than  $4b^{1/2}\lambda \simeq 1.7\lambda$  GeV, indicating that meson topological hybrids should be above about 2.3 GeV, baryon topological hybrids above 2.8 GeV, and pure glue topological hybrids about 1.7 GeV above the  $0^{++}$  glue-loop ground state. It therefore seems plausible that in each case vibrational hybrids will be the lowest-lying new states, though it would be desirable to make these arguments more quantitative.

#### E. Multiquark hadrons

We complete our discussion of hadrons in the flux-tube model by considering states with quark content larger than  $q\bar{q}$  and  $qqq$ . In such states we encounter for the first time a situation in which topological mixing must be considered even when all the internal separations in the system are large. This point is illustrated by the example of  $qq\bar{q}\bar{q}$  in the plane configurations shown in Fig. 9. The adiabatic potentials corresponding to these two flux-tube topologies cross at  $x=y$  so the usual quark-model approximation of neglecting all but the lowest adiabatic surface with given quantum numbers must fail here. Such a system therefore cannot be properly discussed without explicit consideration of topological mixing: when the two levels approach one another they will certainly mix and repel. Figure 10 illustrates, very schematically, the effect such a mixing might have on the adiabatic surfaces of three of the lowest-lying  $qq\bar{q}\bar{q}$  topologies.

This example makes it clear that the dynamics of multiquark states are highly nontrivial and one should beware of models in which they, like mesons and baryons, are automatically confined. It is also clear that any more de-

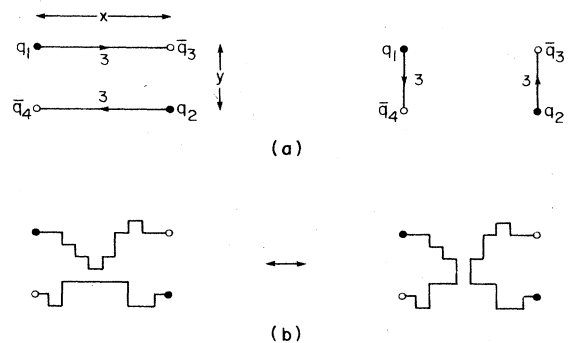


FIG. 9. (a) Two low-lying configurations of  $qq\bar{q}\bar{q}$ . (b) Topological mixing between these two configurations.

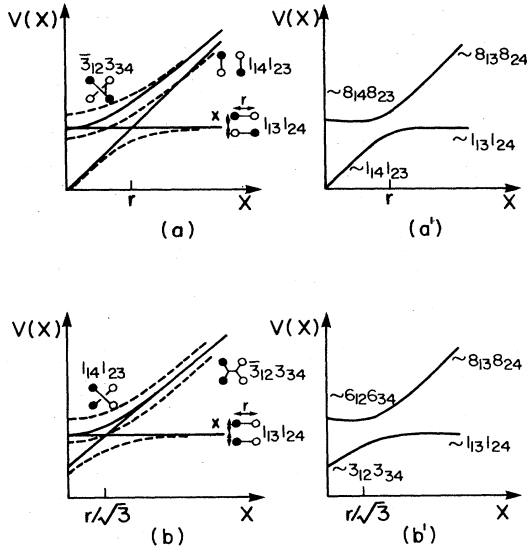


FIG. 10. The adiabatic potentials of the flux-tube model and of the two-body potential for two  $qq\bar{q}\bar{q}$  arrangements: (a) and (b) show the potentials of the model of the text before (shown by solid curves) and after (shown schematically by dashed curves) topological mixing, while (a') and (b') show the related potentials of the two-body  $F_i \cdot F_j$  model used in Ref. 17.

tailed discussion of such states will depend on understanding topological mixing; we will accordingly return to this topic below.

#### IV. MIXING EFFECTS IN THE FLUX-TUBE MODEL

We discuss in this section the two kinds of effects that cause mixing between given topological blocks: flux-tube topological mixing induced by the

$$\frac{1}{ag^2} \sum \text{Tr}[2 - (U_4 U_3 U_2 U_1 + \text{H.c.})]$$

term [as illustrated, for example, in Figs. 7(b) and 7(c)] and quark pair creation (or annihilation) induced by the  $(1/a) \sum q^\dagger U a q$  term [see, for examples, Figs. 6(b) and 6(c)].

##### A. Flux-tube topological mixing

Flux-tube topological mixing can be very important in several situations. Perhaps the clearest case is in the lowest  $q\bar{q}$  adiabatic potential at small  $r < \lambda_0$  where  $g < 1$  and the  $\text{Tr}UUUU$  term becomes very strong. As already mentioned, we know that in this case the effects are very striking: the flux tube with its associated linear potential is converted into a superposition of flux configurations corresponding to an asymptotically free Coulomb's law. Another important example of the effect of this sort of topological mixing occurs when adiabatic surfaces cross; we mentioned a specific case of this type in Sec. III E on multi-quark hadrons.

A more subtle effect of flux-tube topological mixing is to give an internal structure to the flux tube on scales below  $\lambda_0$ . Our model focuses on an imagined lattice spac-

ing  $a \sim \lambda_0$  when discussing the stringlike properties of QCD: with this resolving power the flux tube is stringlike. However, one could imagine studying the flux tube at smaller scales using a lattice spacing  $a < \lambda_0$  for which  $g < 1$ . On such a lattice flux-tube topological mixing would become important and the flux tube would be revealed to have a finite width  $w \sim b^{-1/2}$  inside of which it was "frothy." At a fine enough scale one would discover that the flux tube could allow high-frequency excitations: the gluons of QCD weak-coupling perturbation theory.

Since flux-tube topological mixing is an effect which becomes important for  $g < 1$  where accepting guidance from strong coupling perturbation theory becomes risky, we cannot provide a very quantitative description of this process. Nevertheless, there are some qualitative features of this mixing which we believe we can safely expect and which are sufficient to form a basis for discussing most of its effects. Consider the example of  $qq\bar{q}\bar{q}$  depicted in Fig. 9(a) once again. We would like to know the amplitude for conversion between these two topologies as a function of  $x$  and  $y$ . To estimate this function we first imagine that both  $x$  and  $y$  are much greater than  $\lambda_0$  so that a lattice spacing  $a \sim \lambda_0$  where  $g \sim 1$  can be used to describe the system. In this regime topological mixing is not especially weak, but we can expect that a lowest-order treatment will give a qualitatively sensible picture of the physics. Such lowest-order mixing can occur when the two (discrete) strings find themselves, in the tail of their vibrational wave functions, in a situation where they each have an element occupying a link on opposite sides of an elementary plaquette [see Fig. 9(b)]. They can then mix with an amplitude of order  $1/ag^2 \sim 1/\lambda_0$ . The amplitude that they find themselves ready to mix is, however, damped like a Gaussian in the required displacements of the strings from equilibrium so that even after summation over all of the possible locations for applying the

$$\frac{1}{ag^2} \text{Tr}[2 - (UUUU + \text{H.c.})]$$

perturbation, the mixing will be very small if  $x$  and  $y$  are both much larger than  $\lambda_0$ . Conversely, if there is good overlap between all four relevant string wave functions (the two initial and the two final ones), then this mixing amplitude will be of order  $\lambda_0^{-1} \sim b^{1/2}$  and will be strong.

One of the more interesting applications of these ideas is to the question of long-range forces between hadrons. Using the  $qq\bar{q}\bar{q}$  system of Fig. 9 as a prototype again, we note that if  $y$  corresponds to typical hadronic dimensions and  $x \gg y$ , flux-tube topological mixing between the ground states of the two short (vertical) flux tubes to any states of the two long (horizontal) flux tubes will be suppressed. We conclude that the residual forces between color-singlet hadrons will have no long-range (power-law) tail in this model, in accord with experiment and in contrast to potential models for confinement in which such screening does not occur.<sup>16</sup> (There is, incidentally, a second mechanism which tends to suppress such van der Waals-type forces: flux-tube breaking due to pair creation weakens the effect of the linear potential at large distances and thereby also screens such effects.) Conversely, for distances of the order of 1 fm we can expect

strong topological mixing between color singlets which could lead to molecular-type bound states. Recent calculations,<sup>17</sup> within the context of potential models but including analogous adiabatic surfaces and mixing effects (see Fig. 10), indeed seem to offer insight into the nature of the attractive region of the nucleon-nucleon force along these lines.

### B. Pair-creation effects

Topological mixing can also occur by the creation and annihilation of quark-antiquark pairs via the  $(1/a)q^\dagger U\alpha q$  perturbation. The most important effect of such a term is to allow hadrons to decay, and we devote much of this subsection to a discussion of this process.

Since pair creation is suppressed for large  $a$ , it is, like flux-tube topological mixing, a phenomenon which must be considered at short distance and which is therefore difficult to discuss quantitatively in the strong-coupling picture. In contradistinction to flux-tube topological mixing, however, a simple model for pair creation immediately suggests itself and turns out to be very successful at describing such effects. The model is based once again on considering flux tubes of length  $r \gg \lambda_0$  with a lattice spacing  $a \sim \lambda_0 \sim b^{-1/2}$ . In this case we have the pleasant situation that weak-coupling theory tells us that pair creation is weak for small  $a \ll \lambda_0$  while strong-coupling theory tells us it is weak for  $a \gg \lambda_0$  so that it is plausible that conclusions based on the scale  $a \sim \lambda_0$  may be an excellent guide to the physics.

The obvious model is to assume that pair creation occurs [as in Fig. 6(b)] by breaking the flux tube with equal amplitudes anywhere along its length and in any state of transverse oscillation.<sup>18,19</sup> Thus, for example, a flux tube of length  $r$  in the state  $S$  would decay by pair creation with an amplitude  $\gamma(\xi\mathbf{r},\mathbf{y})$  that is proportional to the string wave function  $\psi^S(\xi,\mathbf{y})$ . Its amplitude to decay to any particular final state would depend on the overlap of the original wave function of the quark and string with two final state quark and string wave functions. An interesting point arises in the derivation of the effective quark pair-creation operator in the flux tube. Since pair creation is only important for  $a \sim \lambda_0$ , it is incorrect to assume that the flux line being broken is oriented along the direction  $\mathbf{r}$ : for such  $a$ , the string flux has become roughened. This means that the line of flux to be broken will have a random orientation and so the pair-creation amplitude  $\gamma(\xi\mathbf{r},\mathbf{y})$  should represent an average over orientations of the amplitude  $(1/a)q^\dagger U\alpha q$ . It is satisfying that this forces one to a pair-creation amplitude which is the local version of the very successful  ${}^3P_0$  model.<sup>20</sup> Moreover, a recent phenomenological study<sup>19</sup> has shown that any residual asymmetry of  $\gamma(\xi\mathbf{r},\mathbf{y})$  along the axis  $\mathbf{r}$  must be quite small: the best fit value for  $\gamma_\perp/\gamma_\parallel$  from this study was  $1.00 \pm 0.02$ , implying only a very small deviation from the spherical value is allowed.

The amplitude  $\gamma_{00}^0(\xi\mathbf{r},\mathbf{y})$  for a ground-state string to break at some point  $(\xi\mathbf{r},\mathbf{y})$  into two ground-state strings is a complicated function. However, it can be shown to be a Gaussian function of  $\mathbf{y}$  with a ( $\xi$ -dependent) width of order  $b^{-1/2}$ . In Ref. 19 it was assumed that  $\gamma(\xi\mathbf{r},\mathbf{y})$  was of

the form appropriate to a flux tube of constant width with "end caps,"

$$\gamma_{00}^0 = \gamma_0 e^{-b^2 \bar{y}^2}, \quad (38)$$

where  $\bar{y}$  is the shortest distance from the point of creation to the line between the quark and the antiquark. Such a model provides an excellent description of meson decay into ordinary mesons in terms of the one free parameter  $\gamma_0$ .

One of the most interesting programs for the future will be to analyze the decays of hybrid mesons into ordinary mesons in the same picture.<sup>21</sup> These parameter-free calculations are essential for understanding the properties of vibrational hybrid mesons and, in particular, may be crucial for designing an experiment to detect such states. We reserve a full discussion of these matters to Sec. VI on phenomenology below, but note here that the amplitude  $\gamma_{00}^1$  for a string in its lowest vibrational mode to break into two ground-state mesons is proportional to the transverse vector  $\mathbf{y}$ . Since  $\mathbf{y}$  carries a unit of axial orbital angular momentum, this means that hybrid mesons cannot, in this approximation, decay into two  $S$ -wave mesons but that they will rather preferentially decay into one  $S$ -wave and one  $P$ -wave meson. This state of affairs has a profound impact on the discussion of the phenomenology of vibrational hybrids.

## V. FURTHER CONSIDERATIONS

### A. Corrections to the adiabatic approximation

The discussion of hadrons in Sec. III was made in the context of an adiabatic approximation. For hadrons containing quarks, in addition to neglecting transitions between different topological sectors, we also neglected transitions between the different adiabatic surfaces  $E^S(r)$  within a given topological sector. The validity of this latter approximation has now been investigated for mesons, and the results are reported in detail elsewhere.<sup>14</sup> This has been done on the basis of a Hamiltonian which generalizes Eq. (15) to include a nonrelativistic kinetic energy term for a quark and antiquark constrained to be on the ends of a string. It is found that the main correction to the discussion of Sec. III A may in fact be regarded not as a breakdown of the adiabatic approximation but rather as corresponding to a change in the form of the adiabatic surfaces in the region where the string energy  $br$  becomes comparable to or larger than the quark masses. One modification is to include a string rigid-body moment of inertia in the centrifugal-barrier term of the effective radial Hamiltonian, i.e., the term

$$\frac{L(L+1) - \Lambda^2}{2\mu r^2} \quad (39)$$

of Eq. (29) becomes

$$\frac{L(L+1) - \Lambda^2}{2\mu r^2 + \frac{1}{6} br^3} \quad (40)$$

The other alteration in the potential surfaces comes about because (for example) the string vibrational frequency which is  $\pi/r$  for infinitely heavy quarks takes the form

$\pi\Lambda(r)/r$  where  $\Lambda(r)\rightarrow 1$  for  $br \ll M_Q$  and  $\Lambda(r)\rightarrow 2$  for  $br \gg M_Q$ . This latter effect, which is the more substantial, has the result that the hybrid mass estimates of column three of Table I should be regarded as lower bounds (see column five), although the increase is small for heavy quarks ( $\sim 60$  MeV for charmonium). For light-quark systems these effects are more substantial, but even for such systems genuine nonadiabatic effects are quite modest for the lowest few adiabatic surfaces.

The above results provide some justification for the success of the potential model in the quantitative description of heavy quarkonium, and are in accord with the view that, with suitable modification to take account of relativistic effects, it should also provide a qualitative description of light mesons. We note that these nonadiabatic corrections correspond to the non-potential-like behavior of chromodynamics which has been discussed for charmonium<sup>22</sup> in the context of the QCD sum rules as the condition  $M_\psi - M_\psi \ll \omega_{\text{glue}}$ .

It is also possible to examine in a similar way deviations from the adiabatic limit in the glue-loop spectrum although this has not yet been done.

### B. Connection to relativistic string models

It is amusing that attempts at a string description of the phenomenology of hadrons actually predate QCD. We refer to the dual model of Veneziano,<sup>23</sup> put into the form of a relativistic string theory by Nambu and Gotto, and later generalizations of it.<sup>24</sup> The satisfactory quantization of fully relativistic string theories is a difficult problem. Our meson string Hamiltonian (15) may be obtained as a nonrelativistic small oscillation approximation to the Nambu-Gotto string Lagrangian with the boundary condition that the ends of the string are fixed. Apart from these approximations the main difference between our meson spectrum and that of the Veneziano model is the possibility in our model of producing excitations in the quark radial motion, as well as orbital and vibrational excitations. (The vibrational hybrids of Sec. IIIA correspond to the "daughter states" of the Veneziano model.) A model with masses attached at the ends of a Nambu-Gotto string was written down by Chodos and Thorn,<sup>25</sup> but they were unable to quantize this theory. They did, however, obtain from it a classical relation between energy  $E$  and angular momentum  $J$  for purely rotational motion. This relation, which leads for large  $J$  to the result  $E = (2\pi bJ)^{1/2}$  of the Veneziano model, is well approximated by a Hamiltonian in which the string motion is treated nonrelativistically.

Vibrational string excitations have been considered in the context of the relativistic quark-confining string model by Giles and Tye.<sup>9</sup> Their lowest vibrational hybrid potential surface is similar to ours, but we do not agree with the centrifugal barrier and angular momentum assignments they make.

Our model of glue loops may similarly be obtained as a nonrelativistic approximation to the closed dual string, although in its original form<sup>26</sup> the dual string is not oriented. The question of string orientation is discussed in the third part of Ref. 26. If the breathing modes of the relativistic dual string are quantized in a manner analogous to

that of Sec. III B, one finds for the effective radial Hamiltonian

$$H = [(2\pi b\rho_0)^2 + \pi_0^2]^{1/2},$$

the expansion of which, for large  $\rho_0$ , yields our nonrelativistic Hamiltonian with the constant  $\gamma=0$ . The nonrelativistic Hamiltonian for general  $\gamma$  may be obtained from the expansion of

$$H_\gamma = [(2\pi b\rho_0)^2 + \pi_0^2 - 4\pi b\gamma]^{1/2}$$

whose eigenvalues corresponding to  $\psi(0)=0$  are

$$E_n = [4\pi b(2n + \frac{3}{2} - \gamma)]^{1/2}, \quad n = 0, 1, \dots$$

In the third of Ref. 8 it is shown that the closed dual string in 3+1 dimensions has a zero-point energy corresponding to the value  $\gamma = \frac{5}{3}$ , somewhat smaller than the value  $\frac{13}{6}$  we obtained from the nonrelativistic string in the adiabatic approximation.

We should also stress the differences between our approach and those which have sought a relativistic quantum string theory of hadrons. In addition to making simplifying approximations to make the problem of quantum string motion tractable, we have also emphasized that the string picture is in our view only an approximation valid at distance scales  $r \gg b^{-1/2}$ , where topological mixing effects may be neglected. It has been suggested that an exact string representation of QCD is attainable, for example, in the large- $N$  limit. If so its consequences are likely to be qualitatively similar to those presented here. On the other hand, we know that for lattice spacing  $a \ll b^{-1/2}$  excitation of flux in arbitrary group representations will become important. It is quite likely that this cannot be represented by a finite number of string degrees of freedom. Because of the limitation of the string picture to phenomena on a scale  $r \gg b^{-1/2}$  there is in our view no need for the existence of an exact relativistic string representation underlying it.

## VI. PHENOMENOLOGICAL IMPLICATIONS

Discovering experimental evidence for gluonic degrees of freedom in hadron spectroscopy is, in our estimation, the most important outstanding qualitative test for QCD. While definitive statements on many of the predicted characteristics of these states must await the completion of detailed calculations, it is already possible to draw some important conclusions.

### A. Vibrational hybrids

We begin by considering hybrids which contain only  $u$ ,  $d$ , and  $s$  quarks. We have predicted that at around 2 GeV the density of such states will begin to far exceed that of the quark model. In particular, we predict that this inflation will begin with two new 36-plets of meson (with their  $I=1$  states around 1.9 GeV) and two 70-plets of baryons (with their  $S=0$  states around 2.4 GeV). Our detailed predictions for the masses and quantum numbers of these states were given above in Sec. III A. The predicted quantum numbers are certain but, as discussed there, the masses have an uncertainty of roughly 100 MeV.

Although there will be ordinary meson and baryon states in these regions, it is conceivable that the hybrid states could be identified as simply being extra states once all of those expected in the usual quark model<sup>27</sup> have been seen. More likely to succeed, however, is a strategy which focuses on a property peculiar to the hybrids. The most obvious such characteristic, applicable in the case of the meson vibrational hybrids, is that three of the lowest-lying predicted meson nonets have members with exotic  $J^{PC}$  quantum numbers:  $0^{+-}$ ,  $1^{-+}$ , and  $2^{+-}$ . The presence of a resonant signal in one of these channels would be strong evidence for the discovery of a hybrid, so it seems sensitive to begin any experimental search for such states in the  $I=1$  and  $I=0$  meson sectors which can reflect this exotic character.

The next question is obvious: in which final states should one look? It would be natural to look in simple channels like the  $\rho\pi$   $P$  wave, which in its  $I=1$  channel has  $J^{PC}=1^{-+}$ . However, as we stressed above, these states will decay preferentially to one  $S$ - and one  $P$ -wave meson so that these double- $S$ -wave channels should be unrewarding.<sup>21</sup> We note that this selection rule could even explain why hybrid mesons have not already been found. In any event, we predict that hybrid mesons will couple most strongly to a series of final states which, so far as we are aware, have not been very thoroughly explored. These dominant decay modes are given in Table III, but we would like to make several supplementary comments. It is clear from the table that the sighting of these states may not be easy. One immediate worry is that the  $1^{-+}$  states, which all have  $S$ -wave decays with generous phase space, may be too broad to be readily seen. In many other cases the favored final states contain a  $P$ -wave meson (such as the  $A_1$ ,  $H$ ,  $Q_1$ , and  $Q_2$ ) which were themselves broad and difficult to detect. Nevertheless, there are some channels, such as  $B\pi$ , which should be clear even if difficult (recall  $B \rightarrow \omega\pi$ ,  $\omega \rightarrow 3\pi$ , so this is a  $5\pi$  final state). Of course at this stage there is also no guarantee that the coupling to a specific allowed mode will be sizable; better advice on where to look must therefore await calculations of the actual widths.<sup>21</sup> At the same time the likelihood that many of these states are very broad further alleviates any difficulty with the fact that they have not already been seen.

Without the help of exotic quantum numbers, hybrid

TABLE III. The dominant decay modes of the exotic hybrids.

$I$	Meson		Favored final states ( $P$ wave $S$ wave) $_L$
	$J^P$	$G$	
1	$2^+$	+	$(A_2\pi)_P, (A_1\pi)_P, (H\pi)_P$
0	$2^+$	-	$(B\pi)_P$
$s\bar{s}$	$2^+$	-	$(K^*(1420)\bar{K})_P, (Q_1\bar{K})_P, (Q_2\bar{K})_P$
1	$1^-$	-	$(B\pi)_S, (D\pi)_S$
0	$1^-$	+	$(A_1\pi)_S$
$s\bar{s}$	$1^-$	+	$(Q_1\bar{K})_S, (Q_2\bar{K})_S$
1	$0^+$	+	$(A_1\pi)_P, (H\pi)_P$
0	$0^+$	-	$(B\pi)_P$
$s\bar{s}$	$0^+$	-	$(Q_1\bar{K})_P, (Q_2\bar{K})_P$

baryons will be more difficult to sort out from the “background” of ordinary baryons. However, it may prove useful in searching for them to consider that they may also decay preferentially to negative-parity baryons of the  $[70,1^-]$  supermultiplet with a ground-state meson and to  $P$ -wave mesons with a ground-state baryon.

Our comments up to this point have concentrated exclusively on hybrids made of the SU(3) quarks  $u$ ,  $d$ , and  $s$ . Of course such states will occur in every flavor sector and in Table I we explicitly show our predictions for the  $b\bar{b}$  and  $c\bar{c}$  systems. These systems are particularly interesting because the physics of the ordinary quark-model states is better understood for them and also the experimental situation is considerably cleaner. Unfortunately, it does not seem likely that the low-lying vibrational hybrids will be more easily seen in these sectors. The  $J^{PC}=1^{--}$  states are not only above the strong decay threshold but they will also have a suppressed direct production since the centrifugal barrier in (29) forces the quark-antiquark wave function to vanish at the origin. It would therefore seem that such states could only be seen in hadronic production decaying to  $P$ - and  $S$ -wave charm or  $b$ -flavor mesons; given the fact that no such  $P$ -wave mesons have yet been seen, this approach would appear to be very difficult.

While  $e^+e^-$  colliders may be unable to directly produce the low-lying  $c\bar{c}$  or  $b\bar{b}$  hybrids, we note in concluding this subsection that the limited number of  $e^+e^- \rightarrow$  three-jet events may be a useful production mechanism for ordinary hybrids: the fragmentation of the (perturbative) gluon should lead to such states, so that a cut on planar events should produce an enhanced sample of hybrids. Of course it is unclear if they can be seen against the combinatorial background in such events. In contrast, in hadronic collisions there is no such signal for events which might contain hybrids, but in compensation they should be produced copiously with typical hadronic cross sections above threshold.

## B. Glue loops

Guidance to the phenomenology of glue loops is much harder to provide. In the first place their masses are much more uncertain: with the present calculational limitations of the model, the whole spectrum can be displaced by a constant, and uncertainties regarding short-range interactions and the (here more dubious) adiabatic approximation make our excitation energies considerably more uncertain than our absolute masses in meson hybrids. Glue loops are also less helpful in providing exotic quantum numbers which would single them out from ordinary mesons: the first exotic states with  $J^{PC}=0^{+-}$ ,  $0^{-+}$ , and  $2^{+-}$  are not expected until the 3-GeV region. We foresee another difficulty as well. Glue loops decay by a second-order pair-creation process which we expect may be visualized as a decay dominated by a transition through a virtual vibrational hybrid meson. However, we have seen that vibrational hybrids decay preferentially to final states with excited mesons. Thus once again it may be ill advised to look for pure glue states in the apparently most natural channels such as  $\pi\pi$  and  $K\bar{K}$ . This, and the high predicted masses of most glue loops, may account for why they have not yet been seen. Indeed, our model leads us to

believe that it may be easier to find hybrid mesons than pure glue states.

We close this section by observing that lattice Monte Carlo calculations of glueball masses may at present also suffer from an uncertainty. If, as we believe, the “universal”  $-13/6\rho$  term in the glue-loop string potential is an artifact, and if present lattices are only small enough to probe the stringlike properties of QCD, lattice glueball masses may be temporarily scaling at values in which this string zero-point effect is playing an important but spurious role.

## VII. FINAL COMMENTS

The flux-tube model we have described here is, it will be apparent, in a rudimentary stage of development. Some features of the model which are crucial to its foundations (e.g., the corrections to the adiabatic limit<sup>14</sup>) or to its phenomenological applications (e.g., the decay widths of vibrational hybrids<sup>21</sup>) are under study, but much remains to be done in both areas.

### A. Checking the foundations

It should be possible to check some of the foundations of the flux-tube model at the most fundamental level via direct comparison of various features of the model with results of numerical calculations using (Euclidean) lattice QCD. Among the possible checks that could be or have been carried out are the following.

(1) For static  $3, \bar{3}$  sources well separated on the lattice, in the absence of light quarks, one should see the series of adiabatic potentials  $V^S(r)$ . It is of course now established that the ground-state gluon configuration does indeed correspond to a linear potential at large  $r$ . There are, moreover, indications that the first excited adiabatic surface exists with a shape and excitation energy comparable to our expectations.<sup>28</sup> There have also been indications from lattice studies<sup>29</sup> for the  $-\pi/12r$  term expected from string zero-point motion, indicating that for presently accessible lattice spacings the gluon field is indeed behaving like a string. Another somewhat more primitive indication of stringlike behavior is the existence of what appears to be the string roughening transition for  $g \sim 1$ .<sup>2,8</sup>

(2) The flux-tube model makes predictions for the adiabatic potentials for systems other than  $3, \bar{3}$ . As examples, it predicts that static  $6, \bar{6}$  sources (or any other nonzero triality sources) exhibit an asymptotically linear lowest adiabatic potential with the same slope as  $3, \bar{3}$  (the lowest adiabatic surface for  $6, \bar{6}$  corresponds to the flux-tube topology in which two 3's emerge from the 6, fuse into a  $\bar{3}$  which then carries the flux a large distance to the vicinity of the  $\bar{6}$  where it splits again into two 3's which terminate on the  $\bar{6}$  sink). In contrast, it predicts that triality-zero sources such as  $8, 8$  and  $10, \bar{10}$  will not be confined<sup>30</sup> (for example, for  $8, 8$  the lowest-energy state of the gluon field asymptotically will correspond to a  $3$  and  $\bar{3}$  of flux emerging from each of the 8's and then annihilating in their respective vicinities). A more complicated example of the same type, which could be of some interest to the nuclear force problem, would involve measuring on the lattice the adiabatic surfaces  $V^I(x, y)$  of the  $qq\bar{q}\bar{q}$  system depicted in

Fig. 9. This would check many of the basic features of the model and could in addition be used to measure the strength of the topological mixing at the point  $x=y$  to check that it indeed falls off rapidly for  $x=y > b^{-1/2}$ .

(3) While the flux-tube model framed here is a model for QCD, its basic principles ought to apply to the confining phase of other gauge theories as well. The simplest example is SU(2) where the analogy is very strong, but where there would still be some important differences. For example, since the 2 of SU(2) is self-conjugate, the “glue-loop” spectrum of SU(2) would correspond to that of a nonoriented rather than an oriented string (see the Appendix). All gauge groups SU( $N$ ) with  $N > 3$  are similar to SU(3) in this respect and the excitation spectrum of their lowest-lying “mesons” and “glue loops” would be expected to be very similar to that of QCD. The differences of these spectra from that of QCD is another measure of the importance of topological mixing and topological excitation. Of course the 3-junction of SU(3) becomes an  $N$ -junction in SU( $N$ ) whose termination by  $N$  quarks gives the simplest baryon of SU( $N$ ). [It has been suggested<sup>31</sup> that the presence of the  $N$ -junction between lines of fundamental flux for  $N > 2$  is responsible for a difference in the orders of the finite-temperature phase transitions of SU( $N$ ) gauge theory without quarks for  $N=2$  and  $N > 2$ .]

The limit of SU( $N$ ) as  $N \rightarrow \infty$  ( $g^2 N$  fixed) has been a subject of intense interest,<sup>32</sup> since a weak-coupling analysis shows that the meson spectrum is stable in this limit. This is also seen in the strong-coupling analysis of Sec. II. The transition amplitude of a state of meson topology to one containing two disconnected pieces necessarily involves either the pair-creation amplitude  $q^\dagger U a q$  or the plaquette term

$$\text{Tr}[2 - (UUUU + \text{H.c.})].$$

In the former case the meson decay amplitude is proportional to  $N^{-1/2}$  and in the latter case to  $N^{-1}$ . The leading decay amplitudes for mesons and pure glue states of SU( $N$ ) are indeed proportional to  $N^{-1/2}$  and  $N^{-1}$ , respectively, exactly as in the weak-coupling analysis. Assuming an approximately fixed radius, the flux-tube model of an SU( $N$ ) “baryon” necessarily breaks down at large  $N$  when the mean interquark spacing becomes very much less than  $b^{-1/2}$ . Since topological mixing in the sense we have defined it is not suppressed at large  $N$ , it seems unlikely that there is an *exact* simple string representation in this limit.

It may be worth adding here a few words of speculation about what is superficially the simplest gauge theory of all: pure electrodynamics. In its lattice formulation as a theory with a compact U(1) local-symmetry group, one simply replaces the Casimir operators of Sec. II by squared integers  $n^2$  and the operators  $U^\dagger, U$  by raising and lowering operators of  $n$ . This theory also confines at large  $g$ , but in 3+1 dimensions has a trivial continuum limit as  $g \rightarrow 0$ . The resolution of this paradox is that the lattice theory has a phase-transition point at a critical value of  $g$  separating the confining and nonconfining phases.<sup>33</sup> In 2+1 dimensions this theory is believed to exhibit linear confinement for all  $g$  (Ref. 34). We suggest that a flux-tube model should also give an approximate

representation of the excitation spectrum of the confining phase of the U(1) gauge theory. To our knowledge, the only lattice calculation to date which bears on this question is consistent with this speculation.<sup>35</sup>

We close this survey by noting an apparent paradox which appears when one compares the block sub-Hamiltonians of different gauge theories, for example, in the sector of the simplest meson topology. The sub-Hamiltonian in each has the form of a discretized string, but the wave velocity appears to depend on the specific gauge theory. We believe that the resolution of this problem lies in the observation<sup>36</sup> that, in going to the continuum limit of the lattice Hamiltonian theory, the "velocity" of light gets renormalized, and that to be precise such lattice Hamiltonians should be multiplied by a renormalization constant whose value is only 1 in the limit  $g \rightarrow 0$ .

### B. Other applications of the flux-tube model

There are a number of other applications of the flux-tube model which we have not discussed here. One important omission from our discussion is quark fragmentation and jet formation. Semiclassical models of string dynamics<sup>37</sup> have had considerable success in this area, and it would certainly be interesting to try to use the flux-tube model to correct and elaborate such models. As just one example, we note that the treatment of baryon production in such models is rather *ad hoc*; the flux-tube model provides definite mechanisms which could be applied to the description of such processes.

As a more speculative example, one could imagine discussing hadronic cross sections in this picture. It would be interesting to try to understand such simple empirical relations as

$$\sigma_{\text{total}}(\text{meson-baryon}) \simeq \frac{2}{3} \sigma_{\text{total}}(\text{baryon-baryon})$$

in terms of a picture of interacting flux tubes.

Finally, we mention that it should be possible to study the spin-spin and spin-orbit properties of the long-range interquark potentials in this picture; such forces could play a significant role in hadron spectroscopy.

## VIII. CONCLUSIONS

We believe that the flux-tube model presented here has many attractions as a picture for hadronic physics in QCD which allows one to proceed beyond the naive quark model. While it reduces to this successful model in an appropriate limit, it makes many predictions for new phenomena, such as hybrids and pure glue states. These predictions all appear to us to be phenomenologically sensible and, especially when supplemented in the future with an understanding of various corrections to the crude spectroscopic results presented here and with predictions for decay widths, would seem to offer a reasonable guide to the experimental search for such states. In this regard we have especially emphasized that the new states are unlikely to be seen in the usual decay channels involving two  $S$ -wave final states, and have offered a preliminary sketch of the territory in which they are likely to be found. In addition to experimental tests of the model, we have pointed out several ways in which its basic tenets have been and

can be tested against the rigorous predictions of QCD as deduced by lattice Monte Carlo methods.

Finally, we have discussed, usually in very general terms but occasionally in some detail, the application of the flux-tube model to other phenomena. We believe that it is possible that this model will prove to be useful in discussing QCD in any situation where the physics of confinement dominates.

## ACKNOWLEDGMENTS

We wish to thank R. H. Dalitz for encouragement and comments, N. Parsons for several conversations, and J. Merlin for his help with some of the numerical work. This study was begun, and much of it completed, while N. I. was on research leave in the Department of Theoretical Physics of the University of Oxford. He is grateful to the Department for its hospitality and support and to the Fellows of St. John's College for a Visiting Fellowship which made his stay in Oxford even more pleasant. J.P. is grateful to the Department of Physics of the University of Toronto for its hospitality during the concluding stages of the work, and to the SERC for a travel grant. This research was also supported in part by a grant from the Natural Sciences and Engineering Research Council of Canada.

## APPENDIX: MESON AND GLUE-LOOP QUANTUM NUMBERS AND EFFECTIVE HAMILTONIANS

We quoted in Secs. III A and III B effective Hamiltonians for vibrational meson hybrids and for glue loops of given total orbital angular momentum. We also listed the possible  $P$  and  $C$  quantum numbers of the corresponding states; we come back to these questions here. From a quark-string state defined with respect to a certain axis, the  $\hat{z}$  axis say, one can use operators of finite rotation to produce a state oriented with respect to a different axis. The wave functions of states of definite total angular momentum  $L$  and component  $M_L$  may be obtained in terms of these. It is convenient in this general discussion to use the standard phase conventions of Jacob and Wick for the relation between states oriented along different axes.

In subsection 1 below, we show that the action of the parity operator  $P$  on a hybrid state of total orbital angular momentum  $L$ , component  $M_L$ , total spin  $S$ , component  $M_S$ , and component of angular momentum along its axis

$$\Lambda = \sum (n_{m+} - n_{m-}),$$

where  $n_{m\pm}$  are the mode occupation numbers, is

$$P | LM_L SM_S; q_i \bar{q}_j; \{n_{m+}, n_{m-}\} \Lambda \rangle \\ = \eta_P | LM_L SM_S; q_i \bar{q}_j; \{n_{m-}, n_{m+}\} - \Lambda \rangle \quad (\text{A1})$$

with  $\eta_P = (-1)^{L+\Lambda+1}$ , and that the action of the charge-conjugation operator  $C$  is

$$C | LM_L SM_S; q_i \bar{q}_j; \{n_{m+}, n_{m-}\} \Lambda \rangle \\ = \eta_C | LM_L SM_S; q_j \bar{q}_i; \{n_{m-}, n_{m+}\} - \Lambda \rangle \quad (\text{A2})$$

with

$$\eta_C = (-1)^{L+S+\Lambda} \prod_m [(-1)^m]^{n_{m-} + n_{m+}}.$$

The quark labels are here flavor labels so for quarks and antiquarks of the same flavor,  $u\bar{u}$ ,  $d\bar{d}$ , etc.,  $i=j$  and these states are eigenstates of  $CP$  with eigenvalue  $\eta_C \eta_P$ , which is thus for ordinary mesons, with all  $n_{m+} = n_{m-} = 0, (-1)^{S+1}$  as usual. We have  $CP = (-1)^S$  for the lowest hybrids with one  $m=1$  phonon, leading to, among other possibilities, the exotic quantum numbers  $J^{PC} = 0^{+-}, 1^{-+}, 2^{+-}$ . The complete set of quantum numbers corresponding to one  $m=1$  phonon are for  $S=1$ ,  $J^{PC} = 2^{+-}, 2^{-+}, 1^{+-}, 1^{-+}, 0^{+-}, 0^{-+}$ , and for  $S=0$ ,  $J^{PC} = 1^{++}, 1^{--}$ .

In subsection 2, we obtain the corresponding result for the  $J^{PC}$  quantum numbers of the glue-loop states.

### 1. Meson vibrational hybrids

Consider first the quark and antiquark at the positions  $(r/2)\hat{z}$  and  $-(r/2)\hat{z}$  along the  $\hat{z}$  axis, with spin components  $s, \bar{s}$ , respectively, with respect to an independent fixed axis. (In order to work in the normal spin-orbital basis of the nonrelativistic quark model, we shall *not* rotate the quark spins when we rotate the quark string system.) We define complex basis vectors

$$\hat{e}^{\pm} = \frac{1}{\sqrt{2}}(\hat{x} \mp i\hat{y}) \quad (\text{A3})$$

$$\begin{aligned} \langle \psi_{s\bar{s}}(rLM_L) | \psi_{s\bar{s}}(\mathbf{r}) \rangle &= \sum_{M'_L} \langle \psi_{s\bar{s}}(rLM_L) | R | \psi_{s\bar{s}}(rLM'_L) \rangle \langle \psi_{s\bar{s}}(rLM'_L) | \psi_{s\bar{s}}(r\hat{z}) \rangle \\ &= D_{M'_L L}^{*L}(\phi, \theta, -\phi) C_L^*(r, \{n_{m+}, n_{m-}\}), \end{aligned} \quad (\text{A7})$$

where the angle dependence is in the first factor, a rotation-group-representation matrix, and the second factor is independent of  $M_L$ . It follows that if the spin quantization axis is the  $\hat{z}$  axis then the state with orbital and spin quantum numbers  $L, M_L, S, M_S$  is

$$| \psi(rLM_L SM_S) \rangle = \sum_{s\bar{s}} \langle \frac{1}{2} s \frac{1}{2} \bar{s} | SM_S \rangle \int d^3r | \psi_{s\bar{s}}(\mathbf{r}) \rangle \langle \psi_{s\bar{s}}(\mathbf{r}) | \psi_{s\bar{s}}(rLM_L) \rangle. \quad (\text{A8})$$

Now use Eq. (A5) and normalize by

$$\langle \psi_{s\bar{s}}(\mathbf{r}') | \psi_{s\bar{s}}(\mathbf{r}) \rangle = \delta_{s's} \delta_{\bar{s}'\bar{s}} \delta^3(\mathbf{r}' - \mathbf{r}), \quad \langle \psi(r'L'M'_L S'M'_S) | \psi(rLM_L SM_S) \rangle = \delta_{S'S} \delta_{M'_S M_S} \delta_{L'L} \delta_{M'_L M_L} r^2 \delta(r' - r),$$

with Kronecker  $\delta$ 's in the suppressed labels for quark flavor and string excitation  $\{n_{m+}, n_{m-}\}$ . Writing out in full the labels of the state vector  $| \psi(rLM_L SM_S) \rangle$  we have

$$\begin{aligned} &| nLM_L SM_S; q_i \bar{q}_j; \{n_{m+}, n_{m-}\} \rangle \\ &= \sum_{s\bar{s}} \langle \frac{1}{2} s \frac{1}{2} \bar{s} | SM_S \rangle \int d^3r \left[ \frac{2L+1}{4\pi} \right]^{1/2} f_{n,L,\{n_{m+}, n_{m-}\}}(r) D_{M'_L L}^L(\phi, \theta, -\phi) \left| q_i \left[ \frac{\mathbf{r}}{2}, s \right] \bar{q}_j \left[ -\frac{\mathbf{r}}{2}, \bar{s} \right]; \{n_{m+}, n_{m-}\} \right\rangle, \end{aligned} \quad (\text{A9})$$

where the radial wave function is

$$f_{n,L,\{n_{m+}, n_{m-}\}}(r) = \left[ \frac{4\pi}{2L+1} \right]^{1/2} C_L(r, \{n_{m+}, n_{m-}\}) \quad (\text{A10})$$

and corresponding complex normal coordinates

$$q_m^{\pm} = \frac{1}{\sqrt{2}}(q_m^1 \pm i q_m^2)$$

so that the string transverse displacement is

$$\mathbf{y}(\xi) = \sum_{\substack{m \\ \sigma=\pm}} \hat{e}^{\sigma} q_m^{\sigma} \sin m \pi \xi. \quad (\text{A4})$$

The states may now be written

$$| \psi_{s\bar{s}}(r\hat{z}) \rangle = \left| q_i \left[ \frac{r}{2}, s \right] \bar{q}_j \left[ -\frac{r}{2}, \bar{s} \right]; \{n_{m+}, n_{m-}\} \right\rangle, \quad (\text{A5})$$

where  $n_{m\pm}$  gives the degree of excitation of the  $m$ th normal mode with  $\sigma = \pm$ . Clearly under a rotation of the quark string system by angle  $\gamma$  about the  $z$  axis this state will just change by a phase factor  $e^{i\Lambda\gamma}$  where

$$\Lambda = \sum (n_{m+} - n_{m-}).$$

To obtain a state  $| \psi_{s\bar{s}}(\mathbf{r}) \rangle$  in a Jacob-Wick-type phase convention we apply a rotation operator:

$$\begin{aligned} | \psi_{s\bar{s}}(\mathbf{r}) \rangle &= R | \psi_{s\bar{s}}(r\hat{z}) \rangle \\ &= e^{-i\phi L_z} e^{-i\theta L_y} e^{+i\phi L_z} | \psi_{s\bar{s}}(r\hat{z}) \rangle \end{aligned} \quad (\text{A6})$$

and we calculate the overlap with a state  $| \psi_{s\bar{s}}(rLM_L) \rangle$  of total orbital angular momentum  $L$ , component  $M_L$ :

normalized to  $r^2 \delta(r' - r)$  and  $n$  is a radial quantum number.

Equation (A9) is the main result of this section. It gives a state of the system with total orbital angular momentum  $L$ , component  $M_L$  as a superposition of adiabatic states with quarks fixed at positions  $\pm r/2$ . To get

an effective adiabatic Hamiltonian for the quark radial motion [the generalization of Eq. (26)] it is simply necessary to find the expectation value in the states of Eq. (A9) of the total Hamiltonian for quark and string motion. This Hamiltonian is obtained in Ref. 14. If it is assumed that the quarks are much more massive than the string, it has the form

$$H = -\frac{1}{2\mu} \frac{\partial^2}{\partial r^2} + \frac{\mathbf{L}_q^2}{2\mu r^2} + E^N(r), \quad (\text{A11})$$

where  $E^N(r)$ , as in Eqs. (24) and (25), is the total energy of the string and  $\mathbf{L}_q$ , the quark angular momentum operator, may be written as  $(\mathbf{L} - \mathbf{L}_S)$ .  $\mathbf{L}$  is the total angular momentum operator and  $\mathbf{L}_S$ , the string angular momentum vector, may be written

$$\mathbf{L}_S = \sum (n_{m+} - n_{m-}) \hat{\mathbf{r}} + \mathbf{L}_{S_1}. \quad (\text{A12})$$

An expression for  $\mathbf{L}_{S_1}$  which raises and lowers the quantum number  $\Lambda$  of  $\mathbf{L}_S \hat{\mathbf{r}}$  is given in Ref. 14. The expectation value of the second term in Eq. (A11) is Eq. (28).

To find the effect of the parity operator  $P$  on the state of Eq. (A9) it is necessary to find the action of  $P$  on the flux-tube state  $|\{n_{m+}, n_{m-}\}\rangle$ . Equations (A3) and (A4) may be generalized to a set of basis vectors  $\hat{\mathbf{e}}_{\mathbf{r}}^{\pm}$  and a string displacement operator  $\mathbf{y}_{\mathbf{r}}(\xi)$  which may be expanded in terms of normal coordinates  $q_m^{\pm}(\mathbf{r})$  by the analog of Eq. (16)

$$\mathbf{y}_{\mathbf{r}}(\xi) = \sum_{\substack{m \\ \sigma=\pm}} \hat{\mathbf{e}}_{\mathbf{r}}^{\sigma} q_m^{\sigma}(\mathbf{r}) \sin m \pi \xi. \quad (\text{A13})$$

From

$$P^{-1} \mathbf{y}_{\mathbf{r}}(\xi) P = -\mathbf{y}_{-\mathbf{r}}(\xi) \quad (\text{A14})$$

$$\begin{aligned} & P | n_L M_L S M_S; q_i \bar{q}_j; \{n_{m+}, n_{m-}\} \rangle \\ &= \eta_q \eta_{\bar{q}} \sum_{\bar{s}} \langle \frac{1}{2} s \frac{1}{2} \bar{s} | S M_S \rangle \int d^3 r f_{n,L, \{n_{m+}, n_{m-}\}}(r) e^{2i\Lambda\phi} \\ & \quad \times D_{M_L \Lambda}^L(\phi, \theta, -\phi) \left| q_i \left[ -\frac{\mathbf{r}}{2}, s \right] \bar{q}_j \left[ \frac{\mathbf{r}}{2}, \bar{s} \right]; \{n_{m-}(-\mathbf{r}), n_{m+}(-\mathbf{r})\} \right\rangle. \end{aligned} \quad (\text{A19})$$

Changing integration variables from  $\mathbf{r}$  to  $-\mathbf{r}$  and using the fact that the radial wave function  $f_{n,L, \{n_{m+}, n_{m-}\}}(r)$  is symmetric under interchange of the string excitation quantum numbers  $n_{m+}$  and  $n_{m-}$ , gives the final result, Eq. (A1).

For the charge-conjugation operator  $C$ , we note that

$$C^{-1} \mathbf{y}_{\mathbf{r}}(\xi) C = \mathbf{y}_{-\mathbf{r}}(1-\xi) \quad (\text{A20})$$

which leads to

$$C^{-1} q_m^{\pm}(\mathbf{r}) C = (-1)^m q_m^{\mp}(-\mathbf{r}) e^{\pm 2i\phi} \quad (\text{A21})$$

so that

$$C | \{n_{m+}(\mathbf{r}), n_{m-}(\mathbf{r})\} \rangle = [(-1)^m]^{n_{m+} + n_{m-}} e^{2i\phi(n_{m+} - n_{m-})} | \{n_{m-}(-\mathbf{r}), n_{m+}(-\mathbf{r})\} \rangle \quad (\text{A22})$$

which leads to Eq. (A2). Combining this with the parity operation we get

it follows that

$$P^{-1} \sum_{\sigma=\pm} \hat{\mathbf{e}}_{\mathbf{r}}^{\sigma} q_m^{\sigma}(\mathbf{r}) P = - \sum_{\sigma=\pm} \hat{\mathbf{e}}_{-\mathbf{r}}^{\sigma} q_m^{\sigma}(-\mathbf{r}) \quad (\text{A15})$$

and since we are using a helicity convention for the flux-tube states we have

$$\begin{aligned} \langle 1\sigma'(-\mathbf{r}) | 1\sigma(\mathbf{r}) \rangle &= \langle 1\sigma'(\hat{\mathbf{z}}) | e^{-i(\pi+\phi)J_z} e^{i(\pi-\theta)J_y} e^{i(\pi+\phi)J_z} \\ & \quad \times e^{-i\phi J_z} e^{-i\theta J_y} e^{i\phi J_z} | 1\sigma(\hat{\mathbf{z}}) \rangle \\ &= -\delta_{-\sigma'\sigma} (-1)^{\sigma} e^{i(\sigma'-\sigma)\phi}. \end{aligned} \quad (\text{A16})$$

This specifies that the basis vectors  $\hat{\mathbf{e}}_{\mathbf{r}}^{\pm}$  and  $\hat{\mathbf{e}}_{-\mathbf{r}}^{\pm}$  are related by  $-\hat{\mathbf{e}}^{-}, \hat{\mathbf{e}}^{+}$  transforming in the same way as  $|1+\rangle, |1-\rangle$ , respectively. So we have from (A16)

$$-\hat{\mathbf{e}}^{-}(-\mathbf{r}) = e^{2i\phi} \hat{\mathbf{e}}^{+}(\mathbf{r}), \quad (\text{A17})$$

$$\hat{\mathbf{e}}^{+}(-\mathbf{r}) = -e^{-2i\phi} \hat{\mathbf{e}}^{-}(\mathbf{r}),$$

and hence from (A15)

$$P^{-1} q_m^{\pm}(\mathbf{r}) P = e^{\pm 2i\phi} q_m^{\mp}(-\mathbf{r}). \quad (\text{A18})$$

Since this is also true for the creation and annihilation operators of flux-tube excitation, we have finally the result

$$\begin{aligned} & P | \{n_{m+}(\mathbf{r}), n_{m-}(\mathbf{r})\} \rangle \\ &= e^{2i(n_{m+} - n_{m-})\phi} | \{n_{m-}(-\mathbf{r}), n_{m+}(-\mathbf{r})\} \rangle, \end{aligned}$$

where the phase factor is  $e^{2i\Lambda\phi}$ , i.e., parity interchanges positive and negative "helicity" occupation numbers. Hence acting on the full quark-antiquark-flux-tube state, Eq. (A9), the parity operator gives

$$CP |LM_L SM_S; q_i \bar{q}_j; \{n_{m_+}, n_{m_-}\}\rangle = \eta_q \eta_{\bar{q}} (-1)^S \prod_m [(-1)^m]^{n_{m_+} + n_{m_-}} |LM_L SM_S; q_j \bar{q}_i; \{n_{m_+}, n_{m_-}\}\rangle \quad (\text{A23})$$

and the phase factor may be rewritten  $(-1)^{S+1+N}$ , where

$$N = \sum m (n_{m_+} + n_{m_-}).$$

## 2. Glue loops

The procedure here is exactly analogous to that for the meson hybrids, but somewhat simpler because of the absence of quarks. Corresponding to Eq. (A9) we have

$$|JM\{n_{m_\rho+}, n_{m_\rho-}\}\{n_{m_z+}, n_{m_z-}\}\rangle = \int d\Omega D_{M\Lambda}^J(\phi, \theta, -\phi) \left[ \frac{2J+1}{4\pi} \right]^{1/2} |\hat{\mathbf{T}}; \{n_{m_\rho+}, n_{m_\rho-}\}\{n_{m_z+}, n_{m_z-}\}\rangle, \quad (\text{A24})$$

where

$$\Lambda = \sum m (n_{m_\rho+} - n_{m_\rho-} + n_{m_z+} - n_{m_z-})$$

in which  $-$  and  $+$  refer to helicities and  $\rho$  and  $z$  refer to mode types. Under the parity operation,  $P, \hat{\mathbf{T}}$  does not change but the mode shapes do change. We have, using the expansion Eq. (30) for  $\rho$

$$P^{-1} \rho(\Phi) P = \hat{\rho} \left[ \rho_0 + \sum_{m=2} [\alpha_m^\rho (-1)^m \sin m \Phi + \beta_m^\rho (-1)^m \cos m \Phi] \right] - \hat{\mathbf{z}} \sum_{m=2} [\alpha_m^z (-1)^m \sin m \Phi + \beta_m^z (-1)^m \cos m \Phi] \quad (\text{A25})$$

so that

$$P^{-1} \rho_0 P = \rho_0, \quad P^{-1} \alpha_m^\rho P = (-1)^m \alpha_m^\rho, \quad P^{-1} \beta_m^\rho P = (-1)^m \beta_m^\rho, \quad (\text{A26})$$

$$P^{-1} \alpha_m^z P = (-1)^{m+1} \alpha_m^z, \quad P^{-1} \beta_m^z P = (-1)^{m+1} \beta_m^z;$$

the same equations apply to the normal coordinates  $\alpha_m^\rho \pm i \beta_m^\rho$  and  $\alpha_m^z \pm i \beta_m^z$ .

Thus, acting with  $P$  on the glue-loop state we obtain

$$P |JM\{n_{m_\rho+}, n_{m_\rho-}\}\{n_{m_z+}, n_{m_z-}\}\rangle = \prod_{m_\rho} [(-1)^{m_\rho}]^{n_{m_\rho+} + n_{m_\rho-}} \prod_{m_z} [(-1)^{m_z+1}]^{n_{m_z+} + n_{m_z-}} |JM\{n_{m_\rho+}, n_{m_\rho-}\}\{n_{m_z+}, n_{m_z-}\}\rangle \quad (\text{A27})$$

and these states are parity eigenstates. Hence all glue loops with no  $\hat{\rho}$  or  $\hat{\mathbf{z}}$  string excitation have positive parity as do those corresponding to the first  $\hat{\mathbf{z}}$  string excitation. The states corresponding to the first  $\hat{\rho}$  string excitation have negative parity. All states built on given string excitation have the same parity independent of  $J$ .

The action of  $C$  on the glue-loop states changes  $\hat{\mathbf{T}} \rightarrow -\hat{\mathbf{T}}$  and interchanges  $n_{m_\rho+}$  and  $n_{m_\rho-}$  as well as  $n_{m_z+}$  and  $n_{m_z-}$ , i.e., it has similar action to that of parity on the hybrid states. The states will always come in pairs with opposite  $C$  except for the case  $n_{m_\rho+} = n_{m_\rho-}$  and

$n_{m_z+} = n_{m_z-}$ . In these cases, which include the breathing modes and their orbital excitations,  $C = (-1)^J$ .

Finally we note that in describing the orbital excitations at the end of Sec. III B we have taken account of the orientation of the glue loop by assuming that the state got by rotating by  $180^\circ$  about an axis perpendicular to the body  $\hat{\mathbf{z}}$  axis is distinct from any of the states before rotation. For an unoriented glue loop which would presumably be appropriate as a model of states of the spectrum of the gauge group  $SU(2)$ , alternate orbital recurrences would be missing.

<sup>1</sup>The idea of color was introduced by O. W. Greenberg, Phys. Rev. Lett. 13, 598 (1964). The idea that the strong interactions might be described by a non-Abelian gauge theory of color originates in H. Fritzsch and M. Gell-Mann, in *Proceedings of the XVI International Conference on High Energy Physics, Chicago-Batavia, Illinois, 1972*, edited by J. D. Jackson and A. Roberts (NAL, Batavia, Illinois, 1973), p. 135; H. Fritzsch, M. Gell-Mann, and H. Leutwyler, Phys. Lett. 74B, 365 (1973); S. Weinberg, Phys. Rev. Lett. 31, 494 (1973).

<sup>2</sup>For reviews of lattice gauge theories and calculations, see, for example, M. Bander, Phys. Rep. 75, 206 (1981); J. Kogut, Rev. Mod. Phys. 55, 775 (1983); L. Susskind, in *Weak and Electromagnetic Interactions at High Energies*, edited by R. Balian and C. H. Llewellyn Smith (North-Holland, Amsterdam, 1977).

<sup>3</sup>See, for example, N. Isgur, in *Particles and Fields—1981: Testing the Standard Model*, proceedings of the Meeting of the Division of Particles and Fields of the APS, Santa Cruz, Cali-

- fornia, edited by C. Heusch and W. T. Kirk (AIP, New York, 1982), p. 1.
- <sup>4</sup>Hamiltonian lattice gauge theories were introduced via the SU(2) theory by J. Kogut and L. Susskind, Phys. Rev. D **11**, 395 (1975).
- <sup>5</sup>R. L. Jaffe and K. Johnson, Phys. Lett. **60B**, 201 (1976); P. Hasenfratz, R. R. Horgan, J. Kuti, and J. M. Richard, *ibid.* **95B**, 299 (1980); T. Barnes, Z. Phys. C **10**, 275 (1981); T. Barnes, F. E. Close, and S. Monaghan, Nucl. Phys. **B198**, 380 (1982); M. Chanowitz and S. Sharpe, *ibid.* **B222**, 211 (1983); E. Golowich, E. Haqq, and G. Karl, Phys. Rev. D **28**, 160 (1983).
- <sup>6</sup>S. Mandelstam, Phys. Rep. **13C**, 261 (1974).
- <sup>7</sup>N. Isgur and J. Paton, Phys. Lett. **124B**, 247 (1983).
- <sup>8</sup>M. Luscher, Nucl. Phys. **B180**, [FS2], 317 (1981); J. B. Kogut *et al.*, Phys. Rev. D **23**, 2945 (1981); L. Brink and H. Nielsen, Phys. Lett. **45B**, 332 (1973); see also Ref. 2.
- <sup>9</sup>S.-H. H. Tye, Phys. Rev. D **13**, 3416 (1976); R. C. Giles, *ibid.* **13**, 1670 (1976); R. C. Giles and S.-H. H. Tye, *ibid.* **13**, 1690 (1976); **16**, 1079 (1977); W. Buchmüller and S.-H. H. Tye, Phys. Rev. Lett. **44**, 850 (1980). These authors considered the dynamics of a meson string, but reached conclusions very different from ours by neglecting the effects of the string angular momentum. See, e.g., Sec. VIA above.
- <sup>10</sup>By different "topologies" we mean configurations which cannot be continuously transformed into one another, but we do not allow the possibility of "knots."
- <sup>11</sup>H. J. Lipkin, Phys. Lett. **113B**, 490 (1982); O. W. Greenberg and J. Hieterinen, *ibid.* **86B**, 309 (1979); Phys. Rev. D **22**, 993 (1980).
- <sup>12</sup>J. B. Kogut, R. D. Pearson, and J. Shigemitsu, Phys. Lett. **98B**, 63 (1981).
- <sup>13</sup>See Refs. 2 and 8 and references cited therein.
- <sup>14</sup>J. Merlin and J. E. Paton, J. Phys. G (to be published).
- <sup>15</sup>I. Barbour and D. K. Ponting, Z. Phys. C **4**, 119 (1980); J. Carlson, J. Kogut, and V. R. Pandharipande, Phys. Rev. D **27**, 233 (1983).
- <sup>16</sup>See O. W. Greenberg and H. J. Lipkin, Nucl. Phys. **A370**, 349 (1981), for a discussion of this issue.
- <sup>17</sup>K. Maltman and N. Isgur, Phys. Rev. Lett. **50**, 1827 (1983); the  $qq\bar{q}\bar{q}$  system is treated along these lines by J. Weinstein and N. Isgur in Phys. Rev. Lett. **48**, 659 (1982). For a recent discussion in terms of string topological mixing, see P. Mathieu and P. J. S. Watson, Carleton University report, 1984 (unpublished).
- <sup>18</sup>J. Alcock and N. Cottingham, University of Bristol report, 1983 (unpublished).
- <sup>19</sup>R. Kokoski and N. Isgur, University of Toronto report, 1984 (unpublished).
- <sup>20</sup>L. Micu, Nucl. Phys. **B10**, 521 (1969); A. Le Yaouanc, L. Oliver, O. Pène, and J. C. Raynal, Phys. Rev. D **8**, 2223 (1973); **9**, 1415 (1974).
- <sup>21</sup>N. Isgur, R. Kokoski, and J. Paton, Phys. Rev. Lett. **54**, 869 (1985).
- <sup>22</sup>V. Zhakarov, in *High Energy Physics—1980*, proceedings of the XX International Conference, Madison, Wisconsin, edited by L. Durand and L. G. Pondrom (AIP, New York, 1981), p. 1235.
- <sup>23</sup>In addition to Ref. 6, see also the review by J. Scherk, Rev. Mod. Phys. **47**, 123 (1975). Recent progress and possible connections to gauge theories are reviewed by A. Neveu, in *Recent Advances in Field Theory and Statistical Mechanics*, proceedings of the 1982 Les Houches Summer School in Theoretical Physics, edited by J. B. Zuber and R. Stora (North-Holland, Amsterdam, 1984).
- <sup>24</sup>For a discussion of the Nambu-Gotto string, see Ref. 6.
- <sup>25</sup>A. Chodos and C. B. Thorn, Nucl. Phys. **B72**, 509 (1972).
- <sup>26</sup>M. A. Virasoro, Phys. Rev. **177**, 2309 (1969); J. A. Shapiro, Phys. Lett. **33B**, 351 (1970); for later developments of the model see J. Schwartz, Phys. Rep. **89**, 223 (1982).
- <sup>27</sup>See, for example, S. Godfrey and N. Isgur, Phys. Rev. (to be published), for a discussion of the usual  $q\bar{q}$  spectrum.
- <sup>28</sup>L. A. Griffiths, C. Michael, and P. E. L. Rakow, Phys. Lett. **129B**, 351 (1983); N. A. Campbell, L. A. Griffiths, C. Michael, and P. E. Rakow, *ibid.* **142B**, 291 (1984).
- <sup>29</sup>S. W. Otto and J. D. Stack, Phys. Rev. Lett. **52**, 2328 (1984).
- <sup>30</sup>This is just the well known result of the strong-coupling limit.
- <sup>31</sup>A. Patel, Caltech report, 1984 (unpublished).
- <sup>32</sup>G. 't Hooft, Nucl. Phys. **B72**, 461 (1974). For a review see S. Coleman, in *Pointlike Structure Inside and Outside Hadrons*, proceedings of the Seventeenth International School of Subnuclear Physics, Erice, 1979, edited by A. Zichichi (Plenum, New York, 1981), p. 11.
- <sup>33</sup>See the review by Kogut in Ref. 2.
- <sup>34</sup>A. M. Polyakov, Nucl. Phys. **B121**, 429 (1975).
- <sup>35</sup>B. Berg and C. Pangiotakopoulos, Phys. Rev. Lett. **52**, 94 (1984).
- <sup>36</sup>A. Hasenfratz and P. Hasenfratz, Nucl. Phys. **B193**, 210 (1981).
- <sup>37</sup>See, for example, B. Andersson and G. Gustafson, Z. Phys. C **3**, 223 (1980); X. Artru and G. Mennessier, Nucl. Phys. **B70**, 93 (1974); M. G. Bowler, Z. Phys. C **22**, 155 (1983).